JOURNAL OF GEOPHYSICAL RESEARCH, VOL. 92, NO. D4, PAGES 4075–4095, APRIL 20, 1987

The Role of Earth Radiation Budget Studies in Climate and General Circulation Research

V. RAMANATHAN[1]

National Center for Atmospheric Research, Boulder, Colorado

Two decades of near-continuous measurements of earth radiation budget data from satellites have made significant contributions to our understanding of the global mean climate, the greenhouse effect, the meridional radiative heating that drives the general circulation, the influence of radiative heating on regional climate, and climate feedback processes. The remaining outstanding problems largely concern the role of clouds in governing climate, in influencing the general circulation, and in determining the sensitivity of climate to external perturbations, i.e., the so-called cloud feedback problem. In this paper a remarkably simple and effective approach is proposed to address these problems, with the aid of the comprehensive radiation budget data collected by the Earth Radiation Budget Experiment (ERBE). ERBE is a multisatellite experiment which began collecting data in November 1984. The simple approach calls for the estimation of clear-sky fluxes from the high spatial resolution scanner measurements. A cloud-radiative forcing (or simply cloud forcing) is defined which is the difference between clear-sky and cloudy-sky (clear plus overcast skies) fluxes. The global average of the sum of the solar and long-wave cloud forcing yields directly the net radiative effect (i.e., cooling or warming) of clouds on climate. Furthermore, analyses of variations in clear-sky fluxes and the cloud forcing in terms of temperature variations would yield the radiation-temperature feedbacks, including the mysterious cloud feedback, that are needed to verify present theories of climate. Finally, general circulation model results are used to discuss the nature of the cloud radiative forcing. It is shown that the long-wave effect of clouds is to enhance the meridional heating gradient in the troposphere, while the albedo or solar effect of clouds is largely to reduce the available solar energy at the surface. The long-wave cloud-induced drive for the circulation is particularly large in the monsoon regions. Thus it is concluded that analyses of ERBE data in terms of cloud forcing would add much needed insights into the role of clouds in the general circulation. With respect to the future, the scientific need is discussed for continuing broadband measurements of earth radiation budget data into the next century in order to understand the processes that govern interannual and decadal climate trends. Finally, the spectral variations in clear-sky fluxes and cloud forcing and the need for broadband data to obtain the desired accuracies are described.

1. INTRODUCTION

The availability of the Nimbus 7 earth radiation budget (ERB) data [see *Jacobowitz et al.*, 1984*a*] and the recent launch of the Earth Radiation Budget Experiment (ERBE) in 1984 [see *Barkstrom*, 1984] have created a flurry of activity in the use of ERB data for climate research. Three comprehensive review papers [*Ohring and Gruber*, 1983; *Kandel*, 1983; *Hartmann et al.*, 1986] discuss in detail the various applications of ERB data for climate research. Hence in this paper, the focus is only on those issues that are not adequately described in the earlier papers of *Ohring and Gruber* [1983] and *Hartmann et al.* [1986].

Largely because of the pioneering efforts of V. Suomi and his then collaborators at the University of Wisconsin (e.g., T. Vonder Haar and F. House) and at NASA Goddard Space Flight Center (e.g., E. Raschke and W. R. Bandeen), the measurement of ERB data began during the mid-1960s (e.g., *House* [1965]; *Bandeen et al.* [1965]; *Suomi et al.* [1967]; *Vonder Haar* [1968]; *Vonder Haar and Suomi* [1969]; and *Raschke and Bandeen* [1970], to cite a few). The collection of ERB data has been and is being maintained through the 1980s. Although strong scientific arguments can be made for the continuation of ERB measurements indefinitely, the future of the ERB data is at a crossroads. This uncertain future of ERB is largely because accurate measurements of ERB are expensive and scientific arguments to categorize ERB measurements as one of the highest-priority measurement objectives have not been articulated effectively and forcefully. In view of this critical juncture, this paper focuses on the following key issues: (1) the contributions of the past measurements to our understanding of the climate system; (2) the potential contributions of ERBE towards resolution of the outstanding issues; and (3) the scientific case for continuation of the ERB measurements.

2. SCIENTIFIC CONTRIBUTIONS OF THE PAST ERB MEASUREMENTS

The measurements taken during the 1960s and 1970s had a significant role in altering and improving our understanding of the role of radiation in climate and in the general circulation. This paper does not attempt a comprehensive listing of the past accomplishments but focuses on a few important contributions.

2.1. *Determination of Fundamental Climate Parameters*

Planetary brightness. The globally and annually averaged albedo or the brightness of the planet is one of the key climate variables. Until the satellite era, investigators relied largely on model calculations for the albedo. The state-of-the art models [e.g., *London*, 1957; *Katayama*, 1967; *Kondratyev and Dyachenko*, 1971] during the 1960s yielded a global annual average value ranging from 34 to 40% (see *Katayama* [1967],

[1]Now at Department of Geophysical Sciences, University of Chicago, Illinois.

Paper number 6D0471.
0148-0227/87/006D-0471$05.00

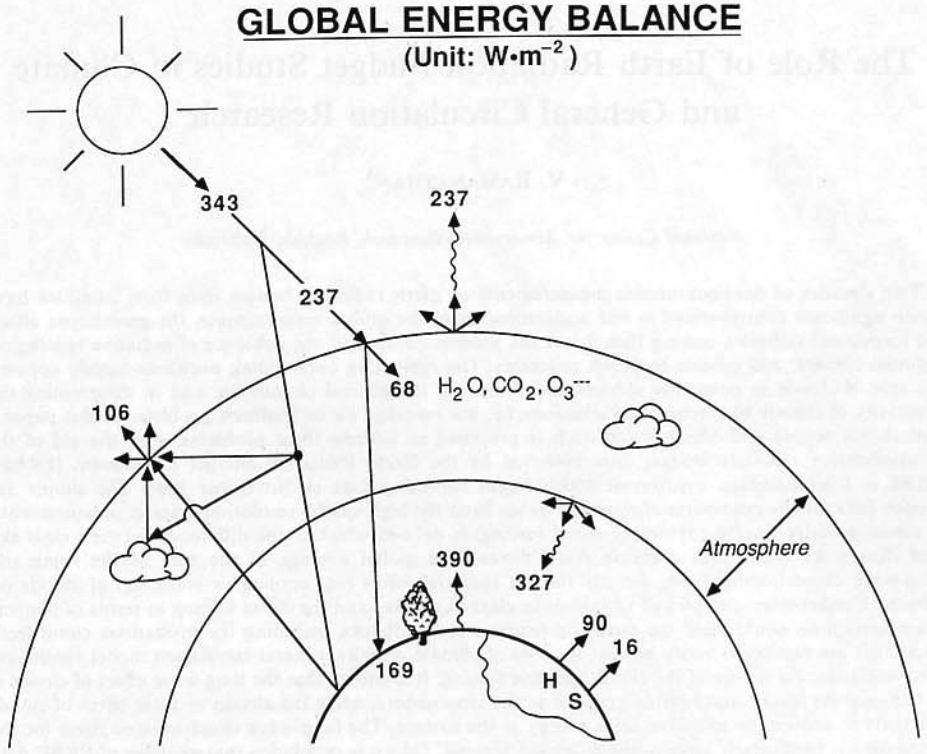

Fig. 1. The global energy balance for annual mean conditions. The top of the atmosphere estimates of solar insolation (343 W m^{-2}), reflected solar radiation (106 W m^{-2}), and outgoing long-wave radiation (237 W m^{-2}) are obtained from satellite data. The other quantities in this figure are obtained from various published model and empirical estimates. The quantities include atmospheric absorption of solar radiation (68 W m^{-2}); surface absorption of solar radiation (169 W m^{-2}); downward long-wave emission by the atmosphere (327 W m^{-2}); upward long-wave emission by the surface (390 W m^{-2}); and H, the latent (90 W m^{-2}), and S, the sensible (17 W m^{-2}), heat fluxes from the surface.

Table 2). As is well known now, satellite estimates revealed the planet to be significantly darker than the theoretical estimates, and the measured values between the various satellites range generally from 29 to 31% (for example, see *Vonder Haar and Suomi* [1971]). The inferences from ERB data that had a tremendous impact on subsequent theoretical studies are (1) the planet is much darker (albedo of about 30%) than pre-satellite era model estimates (~35%), and (2) the annual mean albedo of the two hemispheres is nearly the same (within measurement uncertainty).

The lack of hemispherical asymmetry in the albedo revealed the dominant influence of clouds (over surface effects) in deter-

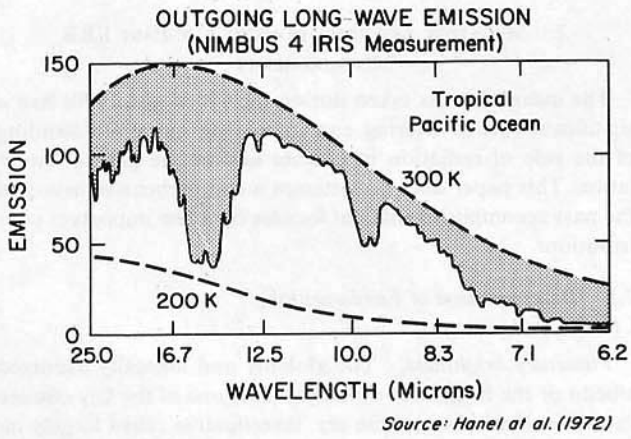

Fig. 2. Spectral distribution of outgoing long-wave emission, as measured by the Nimbus 4 satellite over the tropical Pacific Ocean under clear-sky conditions (source: *Hanel et al* [1972]). Solid line is the measurement. The dashed lines are blackbody curves.

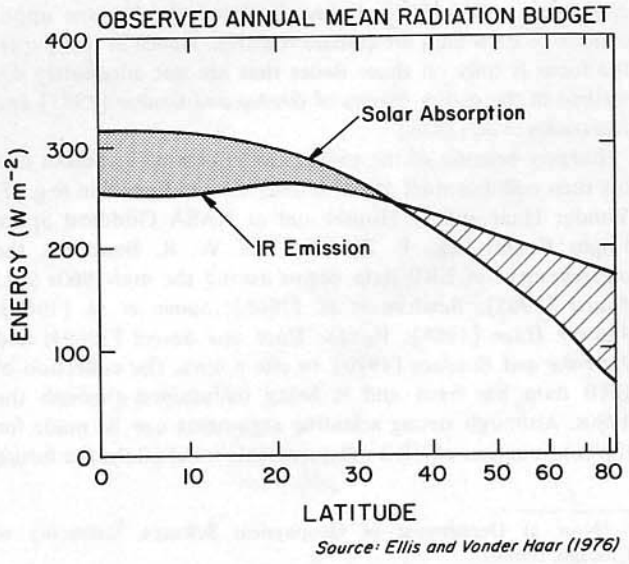

Fig. 3. Annual zonal mean estimates of absorbed solar radiation and outgoing long-wave flux (IR emission) obtained by satellites (source: *Ellis and Vonder Haar* [1976]). Shaded region denotes net heating and dashed regions denote net cooling.

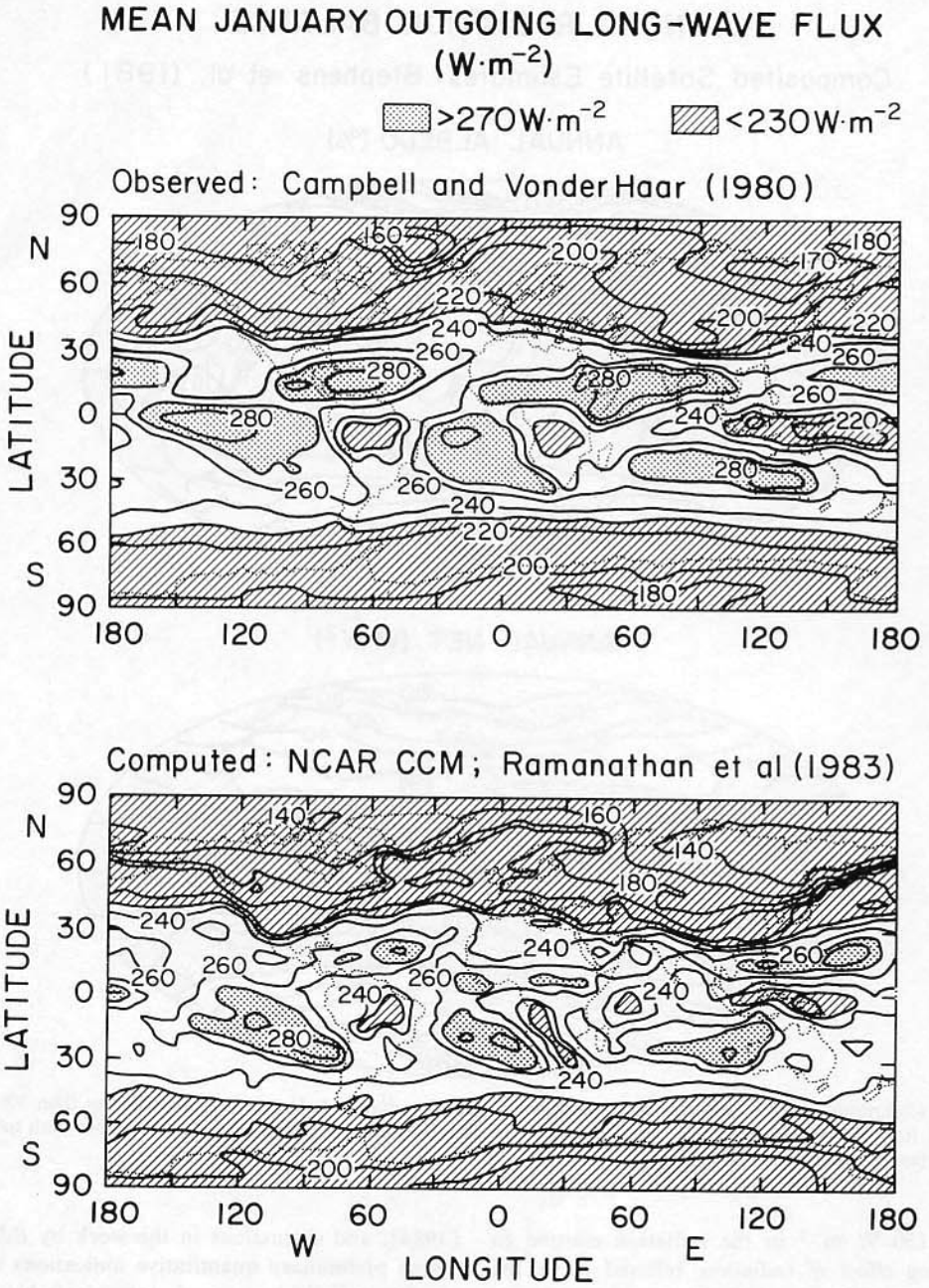

Fig. 4. Outgoing long-wave flux (W m^{-2}) for January. (*a*) Satellite estimates by *Campbell and Vonder Haar* [1980]. (*b*) Model estimates by *Ramanathan et al.* [1983], shown for comparison.

mining the hemispherical mean albedo, since without the cloud effects the significant differences in the surface features between the two hemispheres would have introduced large differences in the hemispherical mean albedo.

Planetary global energy balances. The independent determination of the outgoing (i.e., emitted) long-wave (IR) radiation and the albedo confirmed theoretical expectations and provided new quantitative information. The highlights are given below.

1. On a global annual mean basis, the absorbed solar radiation is in balance with the outgoing long-wave radiation (within measurement accuracy), and the magnitude of the terms shown in Figure 1 is a summary of the various measurements (including Nimbus 7) subjectively obtained by the present author.

2. The balance between solar and long-wave radiation also exists on a hemispherical scale, such that there is no requirement for cross-equatorial energy transport.

The greenhouse effect. The estimates of the outgoing long-wave radiation also lead to quantitative inferences about the atmospheric greenhouse effect. At a globally averaged temperature of 15°C the surface emits about 390 W m^{-2} (see the surface term in Figure 1), while according to satellites, the long-wave radiation escaping to space is only 237 W m^{-2}. Thus the absorption and emission of long-wave radiation by the intervening atmospheric gases and clouds cause a net re-

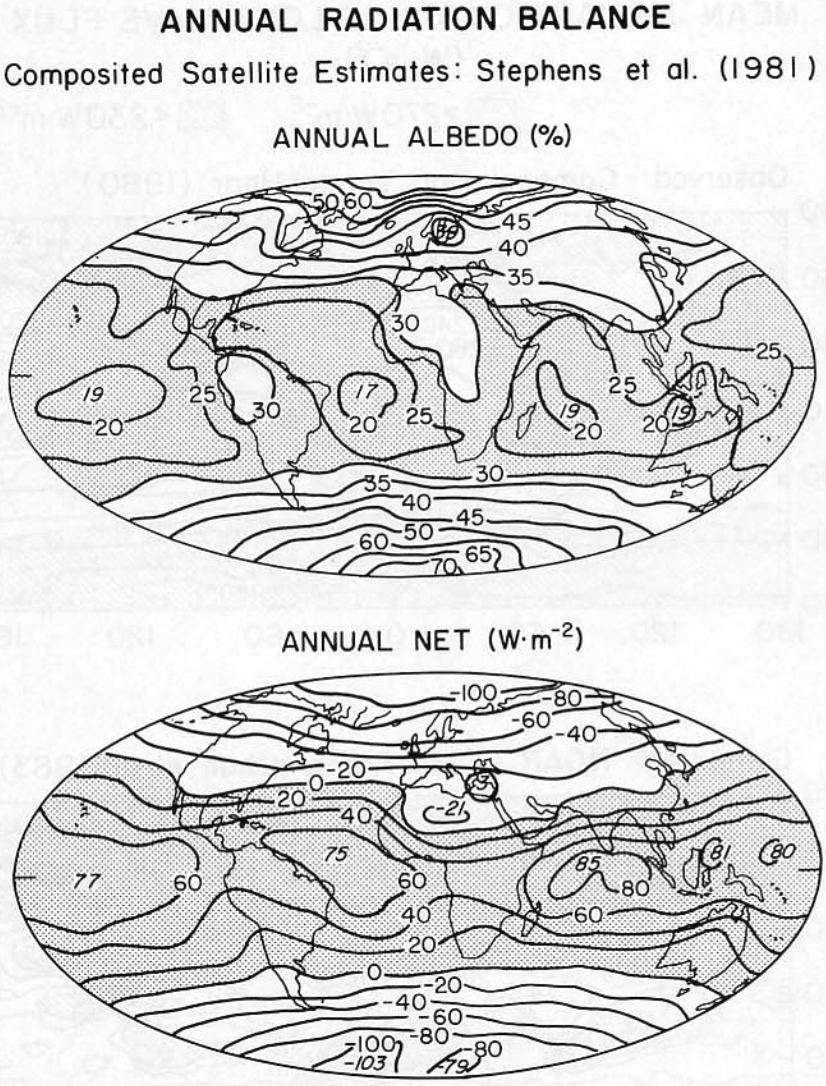

Fig. 5. Composite satellite estimates of annual mean regional radiation balance. Regions with less than 30% albedo are shaded. (top) Albedo; (bottom) Net heating, i.e., absorbed solar minus outgoing long wave. Regions with net heating are shaded (source: *Stephens et al.* [1981]).

duction of about 150 W m^{-2} in the radiation emitted to space. This trapping effect of radiation, referred to as the greenhouse effect, plays a dominant role in governing the temperature of the planet (for example, see *Dickinson* [1985]). This greenhouse effect was revealed more spectacularly in the spectral radiometer on board the Nimbus 4 satellite (see Figure 2). In Figure 2 the smooth curve identified by 300 K is the blackbody emission at the tropical ocean surface. The outgoing radiation reaching space is shown by the irregular curve, and the shaded region indicates the net greenhouse effect. The significant greenhouse effect of CO_2 (15-μm region), O_3 (9.6-μm region), and water vapor (shortwave of 7 μm and long-wave of 16 μm) are clearly seen.

The solar insolation. Accurate determinations of the solar insolation, the so-called "solar constant," and its variations are important because of the potential link of this parameter with climate change [e.g., *Eddy et al.*, 1982]. The active cavity radiometer of the Nimbus 7 ERB instrument revealed high-frequency (2 weeks) variations in the solar insolation of the order of 0.1–0.3% [*Hickey et al.*, 1980]. Furthermore, the Nimbus 7 instruments also seem to suggest an apparent decrease in the insolation of about 0.02% per year (*Wilson* [1984]; and discussions in the work by *Eddy et al.* [1982]). These preliminary quantitative indications are definitely the starting point for a search towards linking climate change with solar variations (also, see *Eddy* [1983]).

TABLE 1. Summary of Estimates of Long-Wave Sensitivity Parameter b

Investigator	b^a
Model Studies	
Budyko [1969]	1.45
Ramanathan [1976]	
fixed cloud-top altitude	2.25
fixed cloud-top temperature	1.37
Coakley and Wielicki [1979]	1.28
Budyko [1975]	1.67
Satellite Studies	
Cess [1976]	1.57
Warren and Schneider [1979]	1.78
Oerlemans and Van den Dool [1978]	2.23
Ohring and Clapp [1980]	1.8

Table adopted from *Ohring and Gruber* [1983].
[a]Here $b = dF/dT_s$ ($Wm^{-2}°C^{-1}$).

TABLE 2. Ice-Albedo Feedback

Model/Investigator	v
Presatellite	
Energy balance model [*Budyko*, 1969]	2.58
Energy balance model [*Sellers*, 1969]	2.17
General circulation model [*Wetherald and Manabe*, 1975]	1.27
Satellite Derived	
Cess [1976]; *Lian and Cess* [1977]	1.25

Source: *Ohring and Gruber*, [1983]. Here v equals amplification due to ice-albedo feedback.

2.2. *Determination of the Forcing Terms of the General Circulation*

Meridional heat transport by oceans and atmospheres. The ERB data revealed that (see Figure 3) on a zonal annual average basis the absorbed solar radiation exceeded outgoing long-wave radiation in the tropical and subtropical regions, resulting in a net radiative heating of the surface-atmosphere column, while the mid to polar latitudes were subjected to a net radiative cooling. This equator-to-pole gradient in radiative heating provides the fundamental forcing for the ocean and atmospheric general circulation. On an annual and long-term mean basis and for the case of zero energy storage and zero temperature change, the net radiative heating must equal the divergence of the meridional energy transport by the oceans and the atmosphere. Based on this consideration, the ERB data were used to derive the meridional transport of energy by the atmosphere and oceans (see *Hartmann et al.* [1986]; also, see original papers by *Rasool and Prabhakara* [1966]; *Vonder Haar and Suomi* [1971]; *Oort and Vonder Haar* [1976]). In addition, observed atmospheric data sets (i.e., temperature and pressure) have been used to estimate the meridional heat transport within the atmosphere, such that results similar to those shown in Figure 3 have been used to infer the oceanic heat transport [*Vonder Haar and Oort*, 1973]. The principal findings are as follows:

1. The maximum meridional heat transport occurs around 30° latitude.
2. In the northern hemisphere the ocean transport contributes roughly 40% of the required heat transport.
3. The inferred total heat transport and, in particular, the oceanic heat transport in the low latitudes is significantly larger (about a factor of 2 in the case of oceans) than earlier empirical and model estimates. The satellite values were larger primarily because the measured tropical albedos were significantly lower than the assumed or computed values of the presatellite era (see further discussions by *Vonder Haar and Oort* [1973]).

Regional forcing (e.g., dynamics of deserts). The measured albedo and the outgoing long-wave radiation revealed significant longitudinal variations. For example, east-west variations in the outgoing long-wave radiation in the tropical regions are as large as equator-to-pole gradients (for example, see Figure 4). These variations have been diagnosed as due to land-sea contrasts in temperatures, humidities, and surface properties and to the preferred regional locations of cloud systems (e.g., marine stratocumulus systems, cloud systems, and tropical cloud clusters). The implications of the regional variations in net radiative heating have not yet been studied in detail, but the data had a major impact on our understanding of the dynamics and maintenance of deserts.

Charney [1975] noted that with the exception of the Sahara desert, the rest of the tropical region is subjected to a net radiative heating (see the bottom panel of Figure 5). The Saharan desert, however, because of the high long-wave emission due to the absence of clouds and the high reflectivity of the desert soil (see top panel, Figure 5), is subjected to a net radiative cooling. The discovery of this feature in the data led *Charney* [1975] to propose the following radiatively induced mechanism for the maintenance of the dryness of the deserts: the radiative cooling of the column is maintained by subsidence warming. The drying effect of the subsidence, of course, maintains the desertlike conditions.

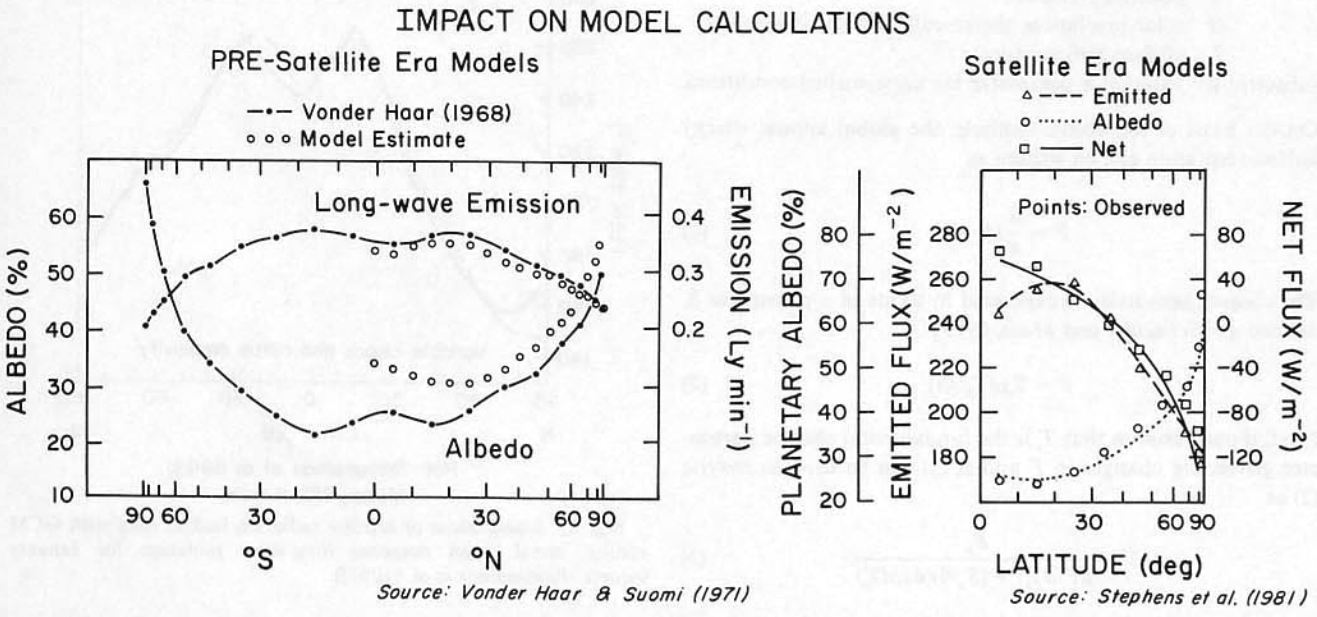

Fig. 6. Comparison of satellite radiation budget estimates with presatellite era (left) and satellite era models (right).

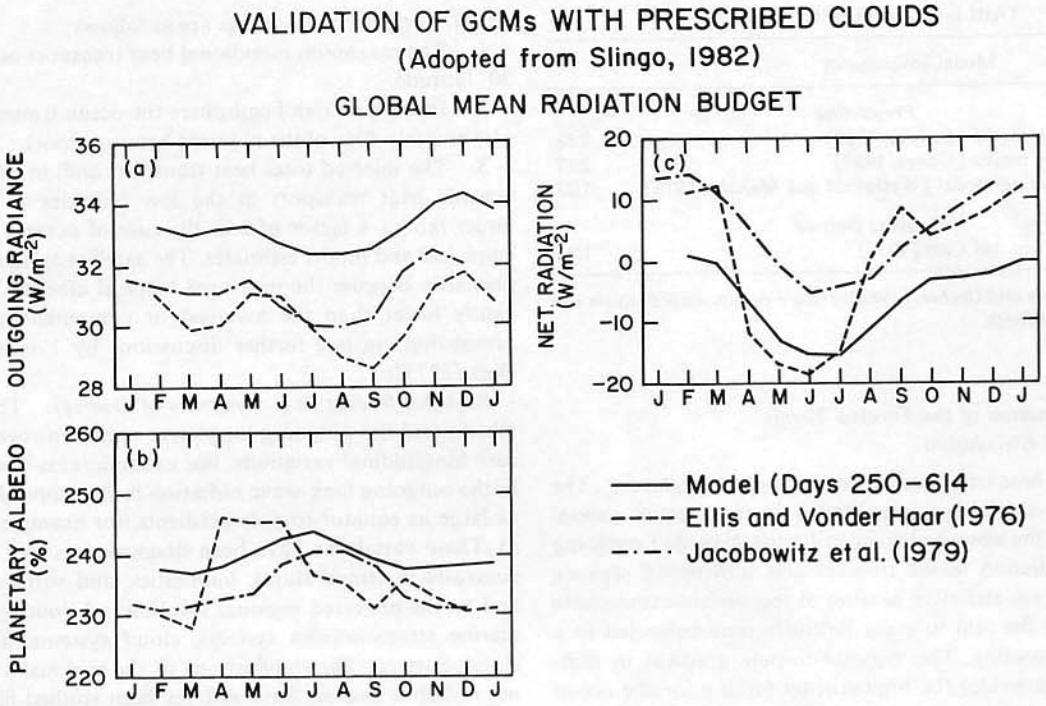

Fig. 7. Comparison of satellite radiation budget data with GCM results: global-annual mean radiation budget (source: *Slingo* [1982]).

2.3. *Climate Feedback Processes*

Satellite data were available for nearly 10 years before the appearance of a pioneering study by *Cess* [1976] which formulated an approach for using ERB data to validate quantitatively the treatment of climate feedback processes in climate models. An exhaustive review of this topic can be found in the work by *Ohring and Gruber* [1983] and hence only a brief summary will be given here. The following symbols are first adopted:

F outgoing long-wave flux;
α planetary albedo;
S solar insolation, the so-called "solar constant";
T_s surface temperature;
subscript u value of a parameter for unperturbed conditions.

On the basis of the above symbols, the global annual energy balance equation can be written as

$$F = \frac{S}{4}(1 - \alpha) \tag{1}$$

The climate sensitivity is expressed in terms of a parameter β, defined as [*Schneider and Mass*, 1975]

$$\beta = S_u(dT_s/dS) \tag{2}$$

Next, if one assumes that T_s is the fundamental climate parameter governing changes in F and α, (1) can be used to rewrite (2) as

$$\beta = \frac{F_u}{(dF/dT_s) + (S_u/4)(d\alpha/dT_s)} \tag{3}$$

Thus the global climate response, as defined by (3), is determined by the infrared (or long wave) feedback parameter (dF/dT_s) and the albedo feedback parameter $(d\alpha/dT_s)$. Before proceeding further the reader should be aware of the conditions for which (3) is valid. Since T_s is assumed to be the

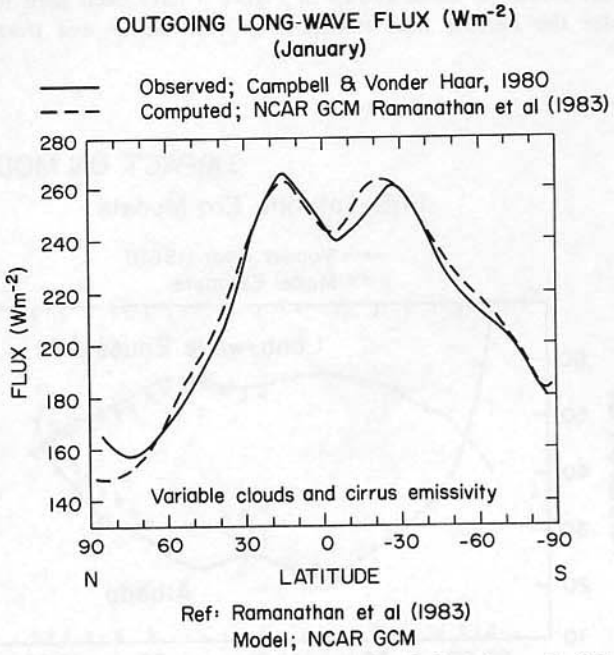

Fig. 8. Comparison of satellite radiation budget data with GCM results: zonal mean outgoing long-wave radiation for January (source: *Ramanathan et al.* [1983]).

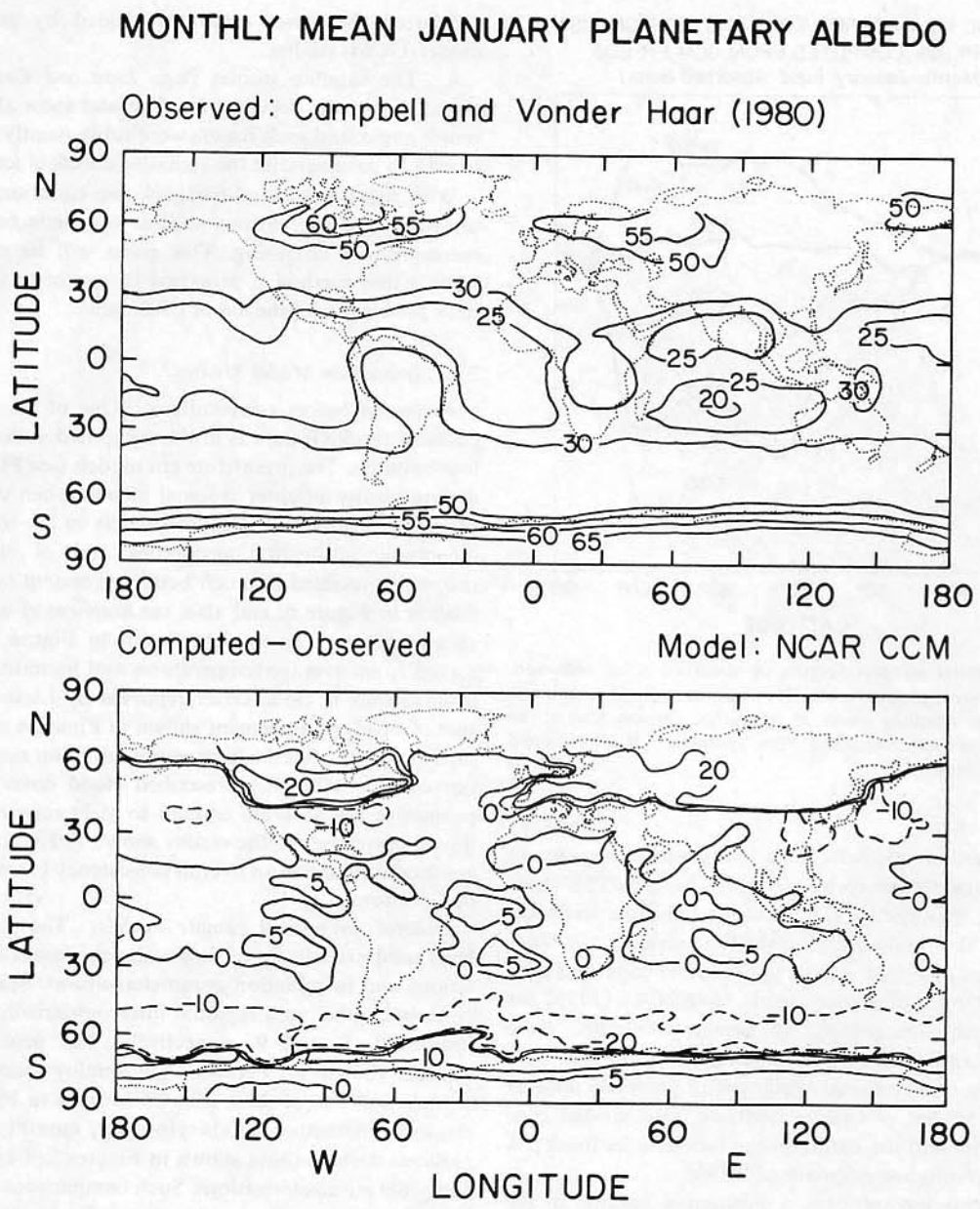

Fig. 9. Comparison of satellite radiation budget data with GCM results: monthly mean albedo for January (source: *Charlock and Ramanathan* [1985]).

fundamental climate variable, (3) is valid only when changes in atmospheric (at least the tropospheric) variables that influence F and α are determined solely, either directly or indirectly, by changes in T_s. This seems to be the case for a large class of problems, such as changes in solar insolation or in CO_2 [e.g., *Ramanathan*, 1977; *Dickinson*, 1985]. However, as shown by *Cess et al.* [1985], there are notable exceptions, such as the "nuclear winter" problem, for which (3) is not a valid approach.

In order to use ERB data to obtain the feedback terms in (3), *Cess* [1976] hypothesized that F and α can be expressed in terms of T_s and cloud cover A_c, i.e.,

$$\frac{dF}{dT_s} = \frac{\partial F}{\partial T_s} + \frac{\partial F}{\partial A_c}\frac{dA_c}{dT_s} \tag{4}$$

Alternately,

$$F = \alpha + bT_s - cA_c \tag{5}$$

with the definition given by (4), (3) can be written as

$$\beta = \frac{F_u}{(\partial F/\partial T_s) + (S_u/4)(\partial\alpha/\partial T_s) + \delta(dA_c/dT_s)} \tag{6}$$

where the cloud-radiation feedback parameter δ is

$$\delta = \frac{S_u}{4}\left(\frac{\partial\alpha}{\partial A_c}\right) + \frac{\partial F}{\partial A_c} \tag{7}$$

In (6), $\partial F/\partial T_s$ is the most important term governing climate sensitivity, and it denotes the (negative) feedback between temperature and humidity changes and long-wave radiation pro-

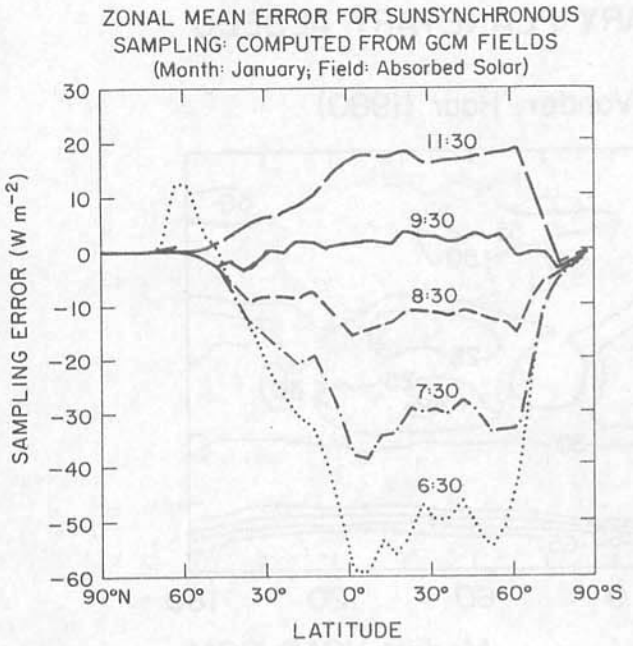

Fig. 10. Potential sampling errors in absorbed solar radiation, inherent in sun-synchronous orbit. The various curves denote the dependence of the sampling errors on equatorial crossing time of the satellite. The errors are computed from synthetic "data" obtained from GCM simulations.

cesses. Contributions to $\partial\alpha/\partial T_s$ largely arise from changes in snow and ice albedo due to temperature changes. This snow and ice albedo response to T_s gives rise to positive feedback, i.e., $(\partial\alpha/\partial T_s) < 0$. Analyses of zonally averaged satellite-measured values of F and α with respect to zonally averaged T_s by *Cess* [1976], and independently by *Budyko* [1975] for $\partial F/\partial T_s$, followed subsequently by numerous studies, have yielded $\partial F/\partial T_s$ and $\partial\alpha/\partial T_s$. These studies, in addition to providing the only observational verification, albeit an indirect one, of model studies of climate feedback, also yielded considerable insights into the nature of the radiative feedbacks. A few of the key results are summarized below.

1. On a zonal average basis a substantial fraction of the meridional variation in F can be explained in terms of the corresponding variation in T_s.

2. The values of $b(=\partial F/\partial T_s$, or dF/dT_s in some cases) derived from satellites were within $\pm 30\%$ of model estimates (see Table 1). This consistency implicitly corroborates the $T_s - H_2O$ water vapor feedback included in models, since without this feedback the model values of b (including those shown in Table 1) would be around 4 W m^{-2} K^{-1} (for example, see *Manabe and Wetherald* [1967]), as opposed to the values of 1.5 to 2.2 W m^{-2} K^{-1} yielded by satellites.

3. Estimates of $\partial\alpha/\partial T_s$ were used by *Cess* [1976] and *Lian and Cess* [1977] to estimate the amplification v of the climate sensitivity by the ice-albedo feedback. These estimates of v, where v is the ratio of the computed β (see equation (3)) with and without the ice-albedo feedback, settled an important issue concerning the importance of this feedback. As shown in Table 2, satellite estimates revealed that the energy balance climate models of *Budyko* [1969] and *Sellers* [1969] had significantly overestimated this feedback. The satellite studies supported the lower estimates yielded by general climate model (GCM) studies.

4. The satellite studies [e.g., *Lian and Cess*, 1977] also revealed a strong dependence of ice and snow albedo on solar zenith angle, and such results were subsequently used in model studies to parameterize the radiative effects of ice and snow.

With regards to cloud feedback (see equation (7)), however, the results of the various studies are inconclusive and, furthermore, are confusing. This point will be discussed later when a new method is proposed to approach the cloud feedback problem with the aid of ERB data.

2.4. *Impact on Model Studies*

Radiation budget computations. One of the significant impacts of the ERB data is in the computed values of albedo in low latitudes. The presatellite era models (see Figure 6) yielded a significantly brighter tropical albedo when compared with satellite measurements. Improvements in the treatment of atmospheric absorption properties and of cloud radiative properties resulted in much better agreement (see satellite era models in Figure 6, and also, see *Stephens et al.* [1981]) with measurements. The models shown in Figure 6 employ observed zonal average temperatures and humidities and surface observations of cloud cover reported by *London* [1957]. The sort of excellent agreement shown in Figure 6 need not necessarily constitute verification of the radiation models, since it is not clear whether the prescribed cloud cover and radiative properties are accurate enough to yield reasonable radiation fluxes. Nevertheless, the results shown in Figure 6 for satellite era models indicate an overall consistency between theory and observations.

General circulation climate models. The ERB data have been used extensively to diagnose deficiencies in model simulations and in radiation parameterizations. Selected examples of global, zonal, and regional intercomparisons are shown in Figures 7, 8, and 9, respectively. The general circulation models shown in Figures 7–9 employ detailed radiation models and one of these (the GCM used in Figures 8 and 9) employs interactive clouds. However, monthly average comparisons such as those shown in Figures 7–9 are not useful to verify the parameterizations. Such comparisons are only useful for validating the simulated radiative forcing that provides the drive for the general circulation. The steps that are needed to verify the parameterizations are outlined in the next section.

In summary, past ERB studies and data have broken new ground in the area of climate research and radiation and climate modeling. The data thus far have provided some of the necessary information to constrain theories and models. A more detailed discussion of these and other uses (e.g., diurnal effects and interannual variability, to name a few) of the data are given by *Ohring and Gruber* [1983], *Hartmann et al.* [1986], and *Kandel* [1983].

3. OUTSTANDING PROBLEMS AND THE ROLE OF ERBE

Although ERB data have been studied extensively for nearly 20 years, there are several important and outstanding scientific problems that remain unsolved. These problems, which will be discussed shortly, will be addressed effectively by ERBE. First, some important issues that concern the measurements themselves will be touched upon.

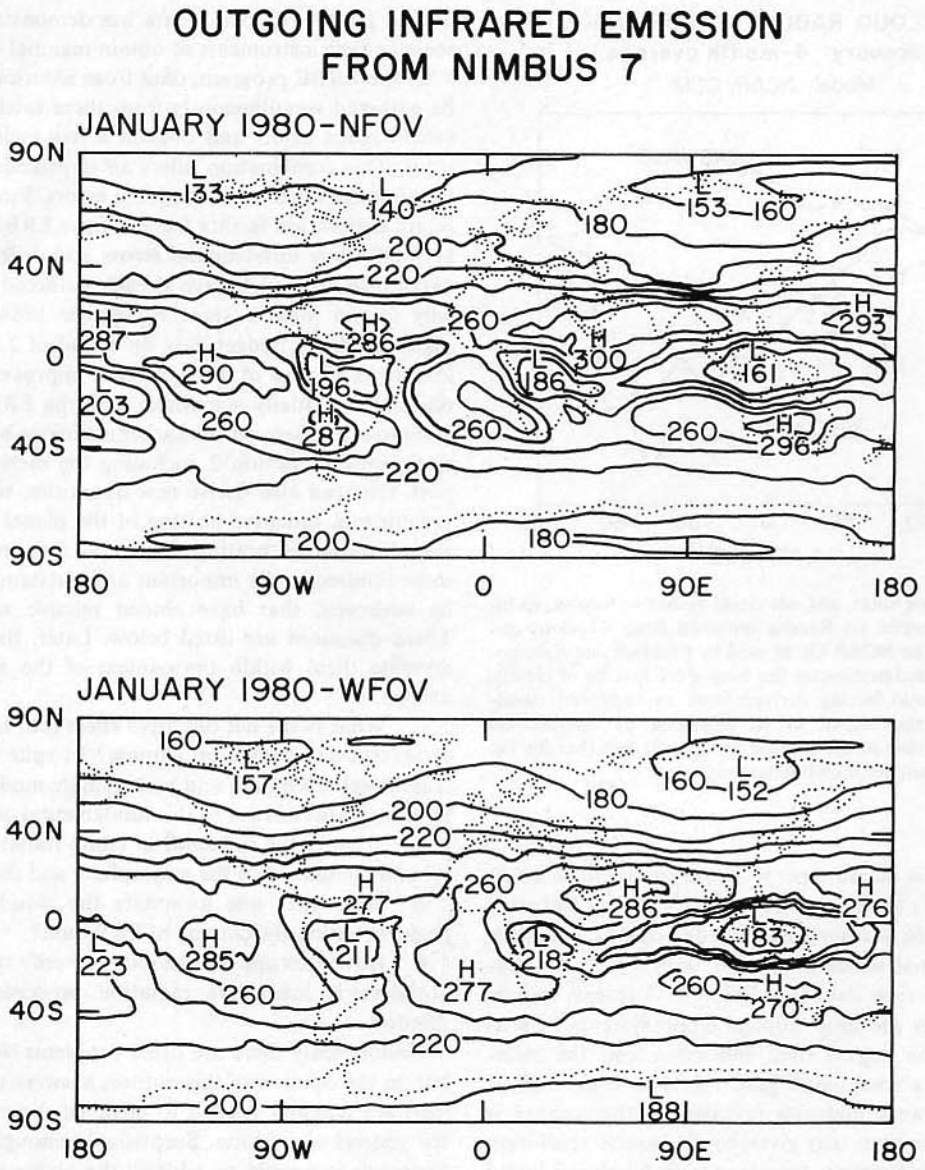

Fig. 11. Comparison of outgoing long-wave or infrared emission, as obtained by a narrow field of view (NFOV), i.e., scanner, instrument and by a wide field of view (WFOV), i.e., nonscanner, instrument on board the Nimbus 7 satellite for January 1980 (source: L. Smith, Colo. State Univ., Fort Collins, private communication, 1986).

There has not been any objective attempt to arrive at uncertainty estimates to the ERB data. Admittedly [see *Jacobowitz et al.*, 1984*b*], it is extremely difficult to assign uncertainty estimates, since these can arise from different sources: uncertainty in the instrument measurement of the radiance, uncertainty in the models that convert the measured radiance to fluxes, uncertainty due to poor diurnal sampling (see *Barkstrom* [1984] and *Barkstrom and Hall* [1982] for further discussion). However, it is generally believed (for example, see *Jacobowitz et al.* [1984*a*]) that poor diurnal sampling is one of the principal sources of uncertainty in earlier measurements, since most of the ERB instruments (e.g., Nimbus 6 and Nmbus 7) were flown on sun-synchronous satellites. Sun-synchronous sampling can potentially introduce a large bias error in the measurement. For example, as shown in Figure 10, simulation studies performed with the aid of a general circulation model (with diurnal cycle) suggest sampling errors that depend systematically on the local time of sampling. The results shown in Figure 10 employ the GCM described by *Ramanathan and Dickinson* [1981]. This model has interactive clouds in six layers from the surface to 18 km in altitude. In the results shown in Figure 10, a "true" daily average radiation budget is obtained by averaging 24 values computed 1 hour apart, and the sampling error is computed by comparing the monthly average of the hourly values with monthly averages of the "true" daily averaged values. Similar results, i.e., systematic bias as a function of local time of sampling, have also been suggested by *Harrison et al.* [1983] and *England and Hunt* [1984], employing narrow-band data taken from geostationary satellites.

The second issue concerns the regional scale of measurements. Most of the earlier measurements, excepting Nimbus 7,

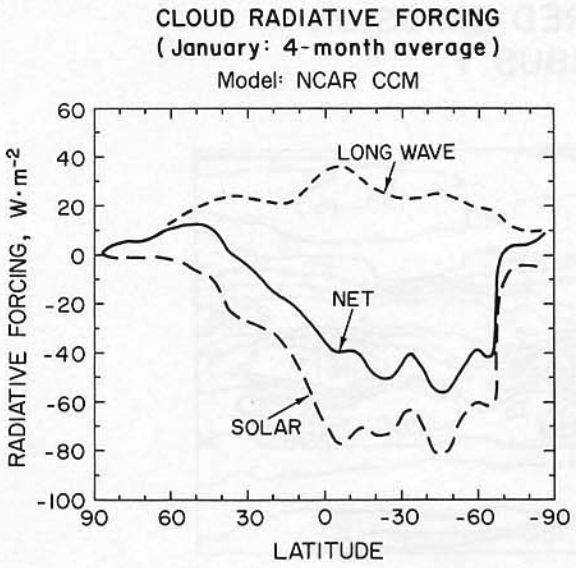

Fig. 12. Long-wave, solar, and net cloud–radiative forcing, as inferred from GCM studies. (*a*) Results obtained from *Charlock and Ramanathan* [1985]. The NCAR GCM used by *Charlock and Ramanathan* [1985] severely underestimates the long-wave forcing of clouds. (*b*) The long-wave cloud forcing derived from an improved cloud-radiative version of the NCAR GCM described by *Ramanathan* [1985]. The cloud forcing of the column (left panel) and that for the troposphere (right panel) are shown separately.

are wide field of view measurements whose spatial scale is too coarse ($\sim(10^3$ km$)^2$) to infer quantitatively regional radiative heating. For example, a comparison of the Nimbus 7 scanner measurements (spatial scales about $(10^2$ km$)^2$) with simultaneous wide field of view data from Nimbus 7 reveals important differences over the deep tropical cloud systems such as the winter monsoon region over Indonesia and the intertropical convergence zone (see Figure 11). Over these regions the outgoing long-wave emission revealed by the scanner is considerably smaller than that given by the coarse resolution measurements. Unfortunately, the scanner on Nimbus 7 lasted only for 18 months [*Jacobowitz et al.*, 1984*b*]. However, the limited period Nimbus 7 data has demonstrated the need for scanner-type instruments to obtain regional energy budget.

In the ERBE program, data from identical instruments will be gathered simultaneously from three satellites, two on sun-synchronous orbits and one on a low-inclination precessing orbit. This combination offers an unprecedented opportunity to minimize the diurnal sampling errors. Furthermore, the on-board calibration facility for all of the ERBE instruments will help minimize instrumental errors and drift. Lastly, the scanners in ERBE (which have already gathered data uninterruptedly for 26 months since November 1984) will furnish the regional energy budget data on a grid of 2.5° latitude by 2.5° longitude. In view of the significant improvements in accuracy that are potentially achievable with the ERBE data, one can, of course, improve on the earlier estimates of all of the parameters listed in section 2, including the meridional heat transport. One can also derive new quantities, such as the diurnal variation in radiative heating of the planet and fine-scale regional radiative heating estimates. But, more importantly, some fundamentally important and outstanding questions can be addressed that have eluded reliable solutions thus far. These questions are listed below. Later, the strategy for addressing them within the context of the ERBE data is described.

1. What is the net radiative effect (i.e., heating or cooling) of present-day clouds on climate? In spite of 20 years of research with ERB data and with climate models, we still do not have a reliable answer to this fundamental question.
2. What is the influence of cloud-radiative forcing on the general circulation of the atmosphere and the oceans?
3. How does one formulate the cloud-climate feedback problem within the context of ERB data?
4. How does one use the data to verify radiation models of atmsopheric long-wave radiation processes and of surface albedo?

Undoubtedly there are other problems that merit attention but, in the opinion of this author, answers to the above problems are urgently needed to advance theories of climate and the general circulation. Surprisingly enough, a rather simple approach is needed to address the above problems with the ERBE data, and this approach is described next.

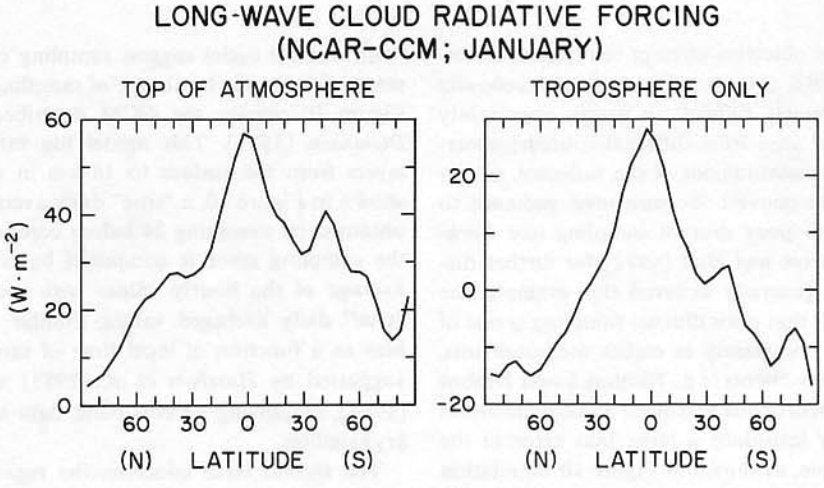

Fig. 12. (continued)

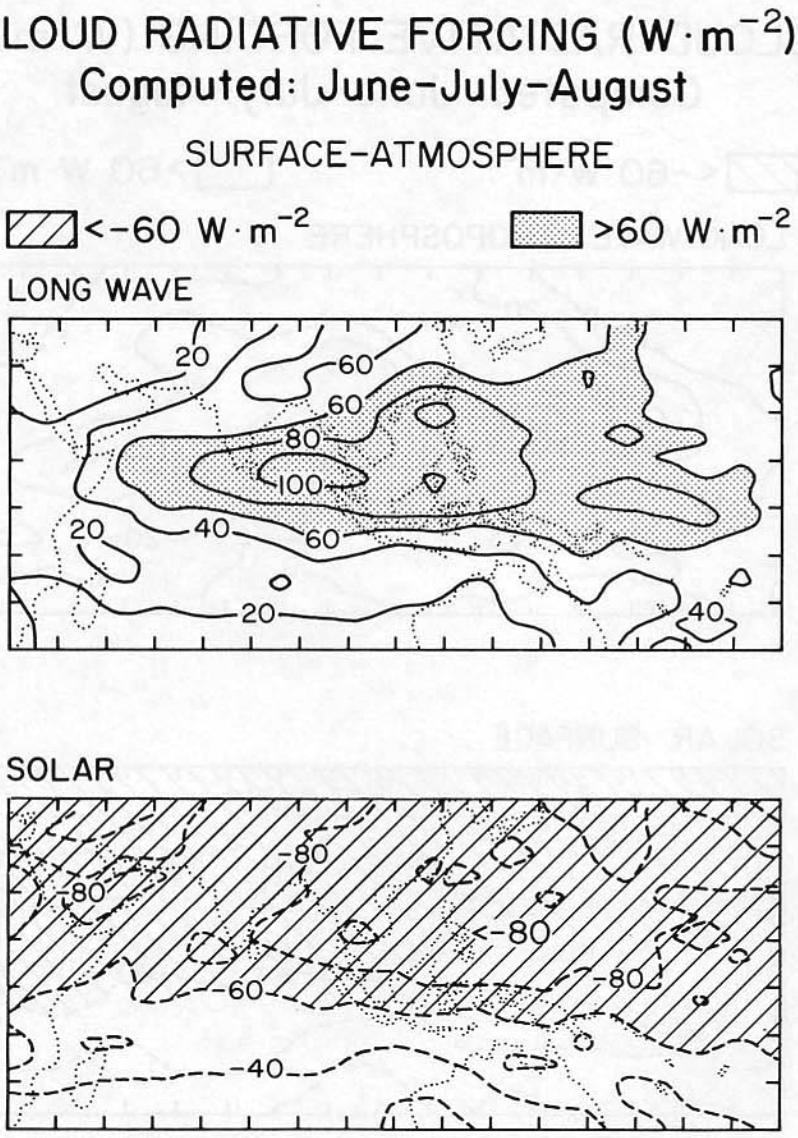

Fig. 13. Computed cloud radiative forcing of the surface-atmosphere column over the Indian subcontinent during the summer monsoon. (Top) long-wave; (bottom) solar. Solid lines indicate positive forcing (heating) and dashed lines indicate negative forcing (cooling).

3.1. *A Simple Approach to Analyzing ERB Data*

Here the outgoing long-wave flux for a unit area with fraction A_c covered by clouds (i.e., A_c is the overcast fraction of the sky) will be considered and the following symbols are defined.

F_c flux from the clear-sky regions;
F_0 flux from the overcast sky;
F cloudy-sky (clear plus overcast) flux;
$C_f(L)$ long-wave cloud-radiative forcing;
A_c cloud-cover fraction.

With the above definitions, one can write

$$F = F_c(1 - A_c) + F_0 A_c \tag{8}$$

$$F = F_c - C_f(L) \tag{9}$$

where

$$C_f(L) = A_c(F_c - F_0) \tag{10}$$

for a single-layer cloud and for scenes with multilevel clouds,

$$C_f(L) = \sum_i A_c{}^i(F_c{}^i - F_0{}^i) \tag{11}$$

where i denotes the region with cloud-cover fraction $A_c{}^i$. The cloud-radiative forcing C_f denotes simply the net effect of clouds in modulating the long-wave radiative flux. To obtain C_f from (11), one needs independent determinations of $A_c{}^i$, $F_c{}^i$, and $F_0{}^i$, a task that is fraught with numerous difficulties. However, C_f can also be obtained from (9) as

$$C_f(L) = F_c - F \tag{12}$$

In (12), F is typically the quantity measured by space-borne

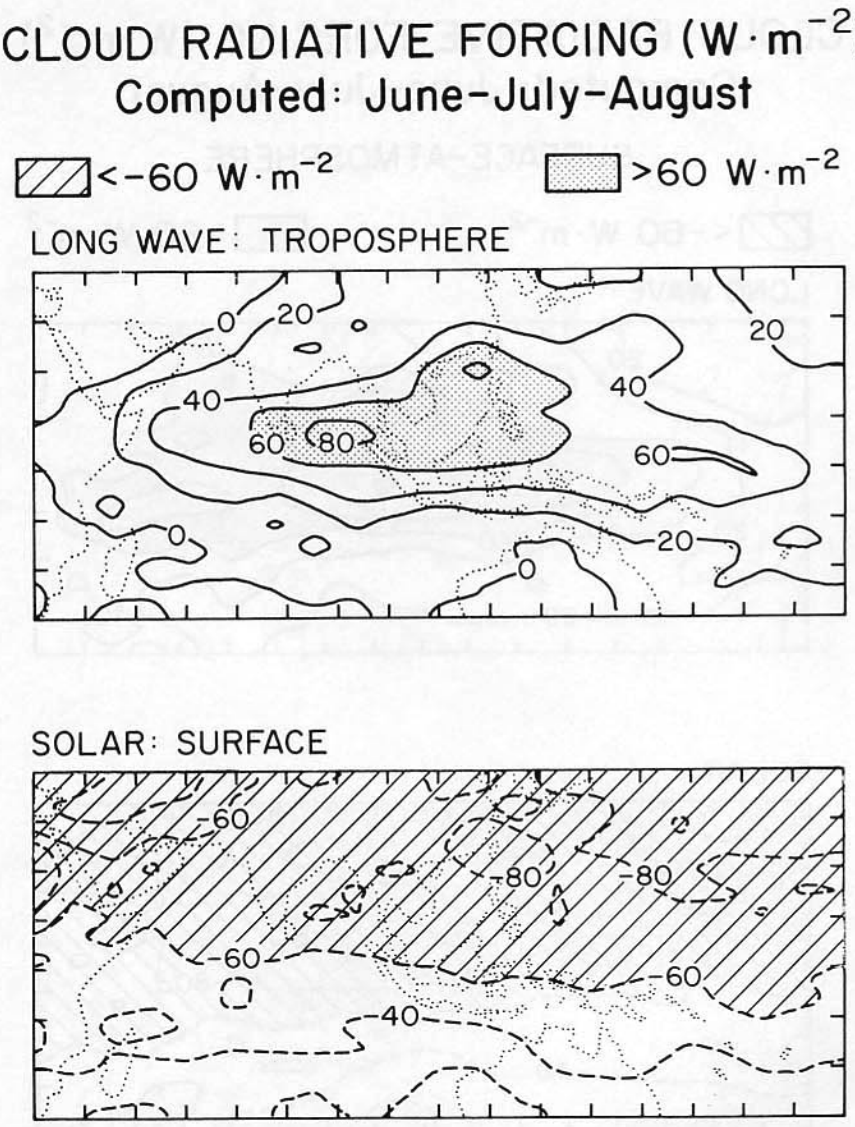

Fig. 14. Same as Figure 13 but separately for the tropospheric heating in the long wave and for the surface heating in the solar.

ERB instruments, be it scanner or wide field of view instruments. The process of obtaining C_f simply reduces to finding a way to infer F_c. Thus the problem of obtaining the cloud effects on climate has reduced to obtaining the clear-sky flux which is a considerably simpler problem when compared with the approach of (11), which involves obtaining cloud-cover fractions and their optical properties.

In ERBE the clear-sky fluxes will be obtained from the scanner data by employing a threshold-type approach. For each 2.5° latitude × 2.5° longitude ERBE grid box, clear-sky regions are identified to be those scanner pixels with the largest outgoing flux and the smallest values of albedo. Roughly 50 partially overlapping scanner pixel measurements within a 2.5° × 2.5° grid box will be available to employ the threshold approach. There are two complications that arise while retrieving F_c from measurements. The first complication arises because of inhomogeneities within the domain (e.g., 2.5° latitude × 2.5° longitude) of interest. As implied in (8) and in (12), the appropriate F_c is the spatially averaged clear-sky flux, that is, the clear-sky flux averaged over all clear-sky scenes within the domain of interest. Such an averaging procedure poses practical difficulties because of the necessity to identify all of the clear-sky scenes. However, this may not be a serious deficiency, since clear-sky fluxes are relatively (relative to overcast skies) homogeneous. The second complication concerns completely overcast skies over the domain. In such instances, estimates of F_c will be unavailable. This difficulty can be overcome by adopting clear-sky estimates taken either prior to or after the occurrence of the overcast skies. If such estimates are unavailable, then we adopt the clear-sky estimates in the surrounding domain.

In suggesting the above practical solutions to the two complications, the spatial homogeneity of clear-sky fluxes on scales ranging from 2.5° to 5° (both in longitude and in latitude) is relied upon. It is important to verify the validity of the homogeneity assumption. For the time being the accuracy of

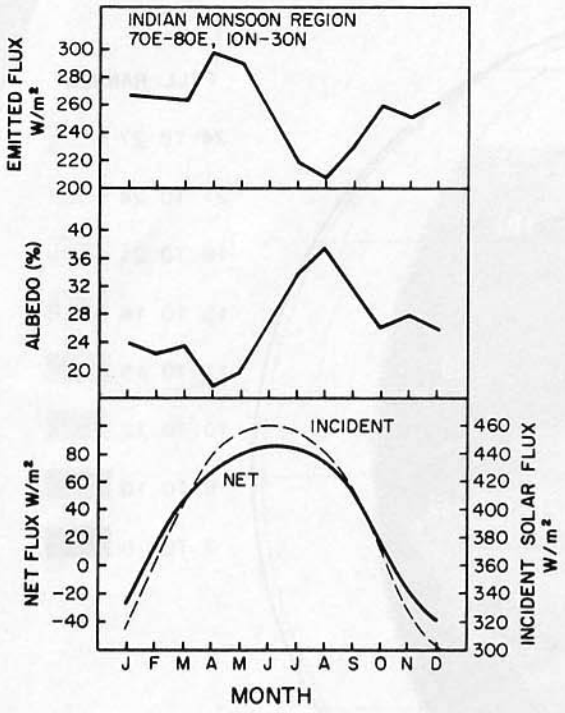

Fig. 15. Satellite estimates of the annual cycle of the planetary albedo, long-wave emission, and net radiative flux for the Asian monsoon region between 70° to 80°E and 10° to 30°N. The annual cycle of the solar insolation is given by the dashed line (source: *Stephens et al.* [1981]).

the clear-sky estimates will be assumed and how one can address the questions raised earlier will be examined.

The above approach of analyzing the data in terms of clear-sky fluxes and cloud forcing has been proposed by *Ellis* [1978], *Ramanathan* [1983, 1985], *Charlock and Ramanathan* [1985], and *Hartmann et al.* [1986]. *Ellis* [1978] obtained clear-sky fluxes and cloud forcing from satellite data, but the accuracies of his clear-sky fluxes were open to question, since he used very coarse resolution ($\sim(10^3$ km$)^2$) data.

3.2. *Net Effect of Clouds on Climate*

Equations similar to (12) can be written for the solar term, such that the net radiative forcing of clouds, $C_f(N)$, can be written as

$$C_f(N) = C_f(L) + C_f(S) \tag{13}$$

where $C_f(L)$ has been defined in (12), and $C_f(S)$ is derived by employing the right-hand side of (1) for absorbed solar flux and is obtained as

$$C_f(S) = \frac{S}{4}(\alpha_c - \alpha) \tag{14}$$

where α is the albedo for the cloudy (clear plus overcast) sky, α_c is the clear-sky albedo, and S is the solar insolation. On the basis of the definitions given in (12) and (14), (13) is obtained from the global energy balance equation (1). Note that, in general, $C_f(L)$ is positive and $C_f(S)$ is negative. The net effect of clouds on climate can be obtained from global average of (13).

At this stage I wish to draw attention to an important difference between this approach and some of the earlier approaches [e.g.: *Ohring and Clapp*, 1980; *Hartmann and Short*, 1980; *Minnis and Harrison*, 1984] of estimating the effect of clouds on the radiation budget. These earlier studies have attempted to estimate the cloud-sensitivity term δ (see equation (7)) by using one of the following forms of δ:

$$\delta = \frac{S_u}{4}\left(\frac{\partial\alpha}{\partial A_c}\right) + \frac{\partial F}{\partial A_c}$$

$$\delta = \frac{\partial F}{\partial A_c}\left[1 + \frac{S_u}{4}\frac{\partial\alpha}{\partial F}\right] \tag{15}$$

$$\delta = \frac{S_u}{4}\left(\frac{\partial\alpha}{\partial A_c}\right)\left[1 + \frac{4}{S_u}\frac{\partial F}{\partial\alpha}\right]$$

These approaches involve estimation of the derivatives $\partial F/\partial A_c$ and $\partial\alpha/\partial A_c$, or correlating changes in F with α to obtain $\partial F/\partial\alpha$. Another form of δ has also been employed [e.g., *Minnis and Harrison*, 1984]. In this approach, one assumes a single-level cloud or an effective single-level cloud, such that (8) can be used to obtain

$$\frac{\partial F}{\partial A_c} = F_0 - F_c \tag{16}$$

Similarly, $\partial\alpha/\partial A_c$ is written as

$$\frac{\partial\alpha}{\partial A_c} = \alpha_0 - \alpha_c \tag{17}$$

and inserting (16) and (17) in (7), δ becomes

$$\delta = (F_0 - F_c) + \frac{S_u}{4}(\alpha_c - \alpha_0) \tag{18}$$

The above δ is also sometimes referred to as cloud forcing [e.g., *Hartmann et al.*, 1986]. In order to avoid further confusions, here the terms estimated by the earlier studies (i.e., $\partial F/\partial A_c$, $\partial\alpha/\partial A_c$, and δ) will be referred to as cloud-radiative sensitivity parameters. In what follows, the significant differences between the cloud-radiative forcing (equations (12)–(14)) and the cloud-sensitivity parameters (equations (15)–(18)) will be summarized.

1. The cloud forcing has a precise definition in that it denotes the radiative heating of the planet due to clouds. The cloud sensitivity indicates the rate of change of the cloud forcing with cloud cover. Since cloud cover is a loosely defined term, the precise definition of the cloud sensitivity is subject to interpretation.

2. The cloud sensitivity involves estimation of either a derivative with respect to A_c (see equation (15)) or the overcast-sky parameters (the terms with subscript 0 in equations (16)–(18)). Estimation of these terms from observed data is fraught with numerous difficulties. In contrast, estimation of the cloud forcing is relatively more straightforward, since it does not involve cloud cover or the parameters for overcast skies.

3.3. *Cloud-Radiative Forcing and the General Circulation*

The influence of clouds on the atmospheric general circulation can best be studied in terms of the cloud-radiative forc-

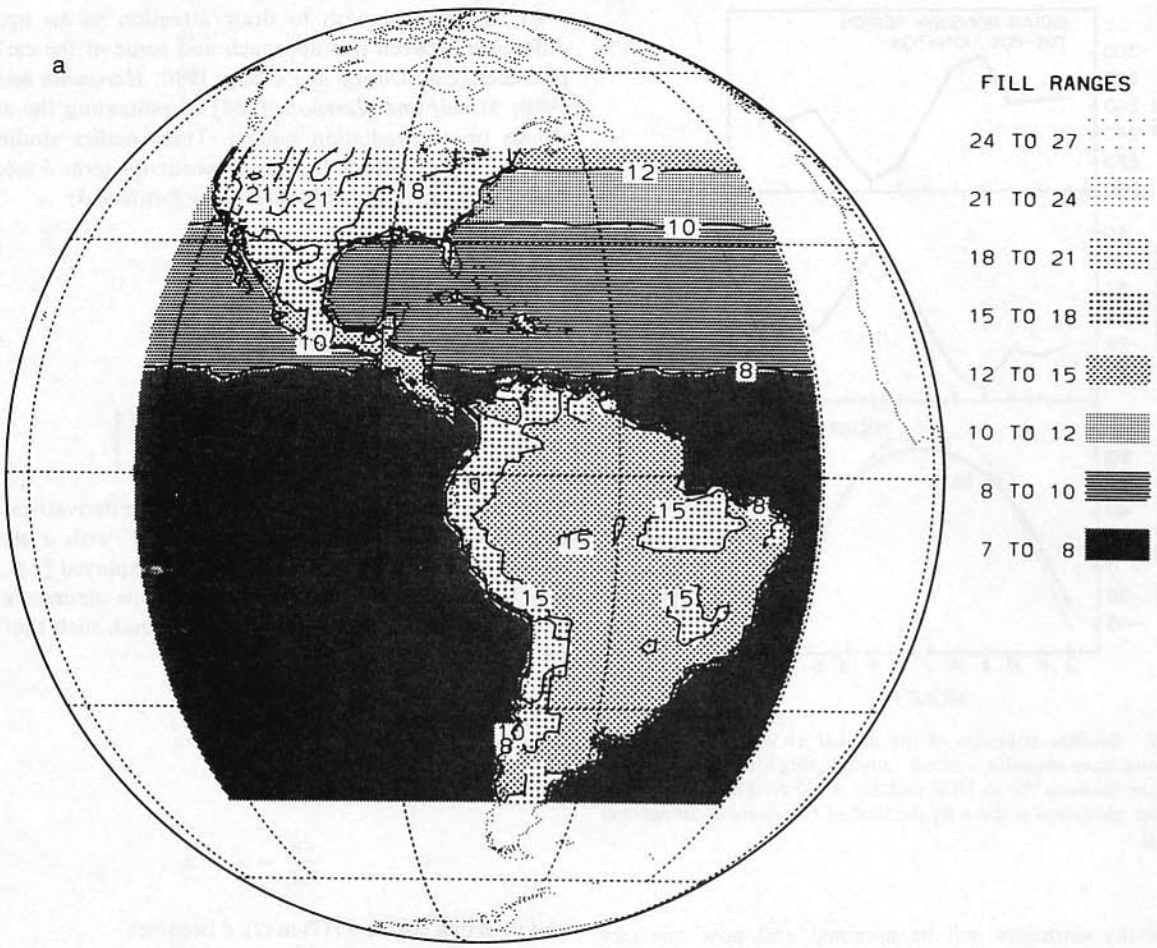

Fig. 16. Comparison of computed clear-sky albedos with those inferred from GOES measurements for noontime in November. (*a*) Observed albedos. (*b*) Computed albedos. (*c*) Computed-observed (source: *Briegleb et al.* [1986]).

ing C_f. Since reliable estimates of C_f from satellite measurements are not available, the potential significance of C_f will be indicated by examining the nature of C_f as obtained from general circulation model studies [e.g., *Ramanathan*, 1983, 1985; *Charlock and Ramanathan*, 1985; *Hartmann et al.*, 1986]. First, it should be pointed out that C_f derived from top of the atmosphere fluxes denotes the cloud forcing for the surface-atmosphere column. The cloud-forcing terms can also be derived for the surface and for the atmosphere if the surface fluxes are known (as in the case of a model). *Charlock and Ramanathan* [1983] and *Hartmann et al.* [1986] described surface-atmosphere forcing, whereas *Ramanathan* [1985] illustrated the cloud-forcing terms for the column as well as separately for the surface and the troposphere. Studies of column radiative forcing by clouds revealed the following significant features (also see Figure 12):

1. Clouds have a large long-wave heating effect and a significantly larger solar cooling effect, particularly in the summer hemisphere (Figure 12*a*). Results similar to those shown in Figure 12*a* were also obtained by *Ellis* [1978]. Ellis' analyses of satellite measurements yielded globally averaged values of 20 W m^{-2} for long-wave cloud forcing, -47 W m^{-2} for solar forcing, and -27 W m^{-2} for the net forcing.

2. The cloud forcing has a strong equator-to-pole gradient. In the long-wave region, clouds enhance the existing meridional heating gradient (Figure 12*b*), whereas in the solar they reduce the gradient.

However, one should be cautious about quickly interpreting the above results in terms of the cloud effects on general circulation. In order to highlight this point, the summer moonsoon season over the Indian subcontinent is examined and the radiative forcing of the column (Figure 13) and that of the troposphere and surface is considered separately (Figure 14). These results were obtained basically from the GCM known as the National Center for Atmospheric Research (NCAR) Community Climate model, as described by *Pitcher et al.* [1983], but with a significantly improved radiation scheme described by *Ramanathan* [1985] and *Ramanathan and Downey* [1986].

The low outgoing long-wave fluxes over the monsoon region are well known (for example, see *Smith* [1984]) which, for (12), implies strong cloud-radiative forcing in the long-wave, as indeed shown in Figure 13. However, the deep monsoon clouds also enhance the albedo, and thus the solar forcing is also large but negative. Thus for the column as a whole the long-wave and solar forcing of clouds are each large, but of opposite sign. Similar results have also been obtained by *Stephens et al.* [1981] from satellite measurements (Figure 15). As shown in Figure 15, the dip in the outgoing long-wave flux

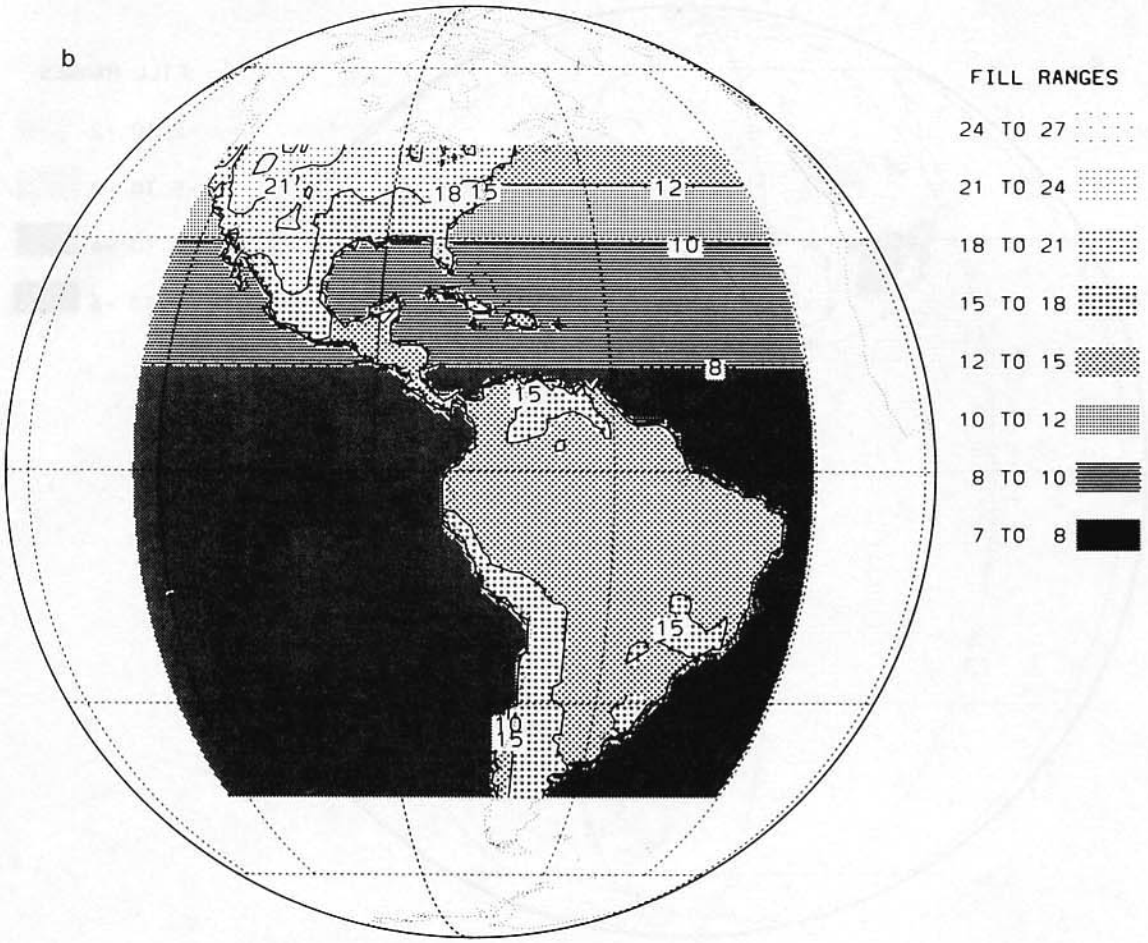

Fig. 16. (continued)

is compensated for by a corresponding rise in the albedo such that the net radiative heating follows very nearly the seasonal course of the incident solar radiation (see the bottom panel in Figure 15).

The above results do not necessarily imply that clouds do not have a net radiative effect on the monsoons. Let us consider Figure 14, which shows the long-wave cloud forcing for the troposphere (top panel) and the solar forcing for the surface (bottom panel). It is seen that roughly 80% of the cloud long-wave heating of the column is manifested in the troposphere (compare the top panels of Figures 13 and 14), while 80–100% of the cloud solar cooling is felt at the surface. Thus the radiative effects of clouds are very similar to that of latent heat release in that they remove heat (solar energy) from the surface and deposit it (as long-wave energy) in the troposphere. The magnitudes (~ 100 W m^{-2}) are significant when compared with either solar heating of the surface in the oceans or the latent heat released in the atmosphere. Results similar to those shown in Figure 14 have also been obtained for the winter monsoon over Indonesia for the month of January [see *Ramanathan*, 1985]. This cloud-induced long-wave heating of the troposphere can influence the monsoon circulation in the following ways:

1. A reverse Charney effect for the deserts, i.e., the heating induces upward motion in the column and the compensatory subsidence in the surrounding regions (thousands of kilometers away) brings in moisture from the oceans to maintain the semipermanent cloud systems.

2. The surface solar cooling effect and the atmospheric long-wave warming effect of clouds will also tend to stabilize the column just as the effect of latent heat release. Thus in tropical deep-cloud systems, radiative effects of clouds may play an important role in maintaining the vertical thermal structure, an effect that has been neglected in previous studies, but one that has also been pointed out by *Houze* [1982]. For example, GCM sensitivity studies by *Ramanathan* [1983] have suggested that the long-wave radiative forcing by black cirrus clouds has a significant warming effect (about 5 K) on the tropical upper troposphere and also has a substantial strengthening effect on the winter and summertime jet stream. In addition, GCM studies by *Shukla and Sud* [1981] have illustrated the potential influence of cloud-radiative interactions in the generation and destruction of eddy kinetic energy.

In summary, the radiative forcing of clouds has a significant impact on the general circulation and satellite estimates (as yet unavailable) of cloud-radiative forcing offer exciting possibilities to provide new insights concerning the role of radiation in the general circulation.

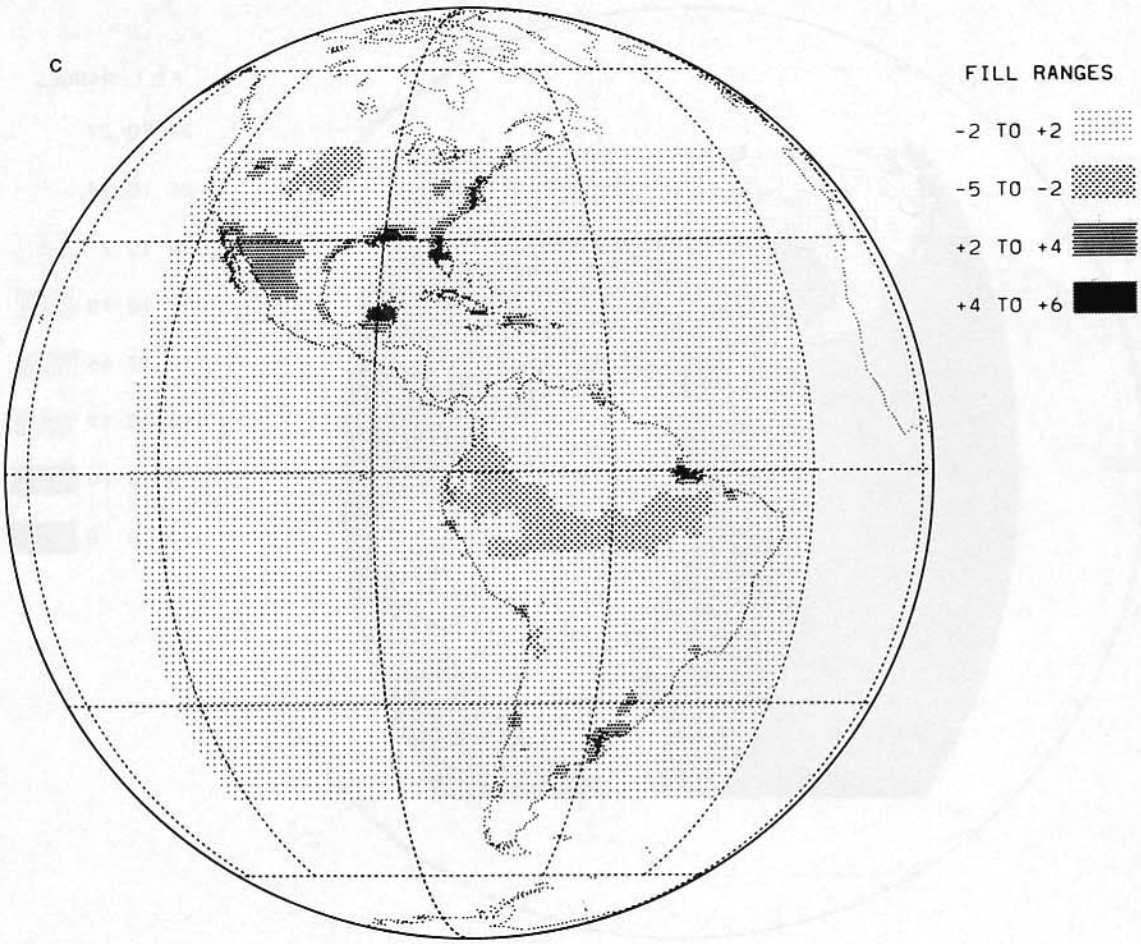

Fig. 16. (continued)

3.4. *A New Approach for Inferring Cloud and Other Radiative Feedbacks*

The analyses of the top of the atmosphere fluxes in terms of clear-sky flux and the cloud-forcing term offers a straightforward way to infer the climate feedbacks from ERB data. On the basis of (8), (12), (13), and (14), the climate sensitivity equation (6) can be rewritten as

$$\beta = \frac{F_u}{(\partial F_c/\partial T_s) + (\partial \alpha_c/\partial T_s) - (\partial/\partial T_s)[C_f(N)]} \tag{19}$$

The main simplicity of (19) is in the cloud feedback term, since, as opposed to (6), the nearly impossible task of evaluating the dA_c/dT_s term need not be undertaken. R. D. Cess (private communication, 1986) has also suggested a similar approach for inferring cloud feedback. Of course, one has to make one of the following hypotheses for evaluating the partial derivatives in the denominator of (19): that the latitudinal change in the fluxes and temperature are influenced by the same processes that govern climate change, or that the seasonal or interannual or decadal changes in the global and zonal mean fluxes and T_s are influenced by the same processes that govern climate change.

By making either of the above hypotheses, one can infer the feedbacks from long-term ($\sim$10 years) records of ERB data through (19). It is important to be aware of the partial derivatives in (19), since the (spatial and temporal) variations in fluxes due to trace gas (e.g., O_3, CO_2, and others) variations, zenith angle (in the case of solar fluxes) variations, and surface parameters, to name a few, should be separated from those arising from temperature and humidity variations (see *Lian and Cess* [1977] for an elaboration of this important point).

3.5. *Model Verification*

The analyses of the data in terms of clear-sky fluxes and cloud forcing facilitates a methodical and objective procedure to verify radiation models and general circulation models. First, such a procedure involves comparison of instantaneous radiances (as opposed to fluxes), followed by comparison of clear-sky fluxes over the globe, leading finally to comparison of the cloud forcing.

Instantaneous radiances. For the long-wave region an approach has been proposed by *Ramanathan and Downey* [1986] for comparing models with ERBE radiances. In this approach, radiosonde soundings of temperature and humidity serve as model input and only those soundings that fall within ± 30 km and within ± 0.5 hour of an ERBE measurement are adopted for the comparison. Furthermore, only homogeneous

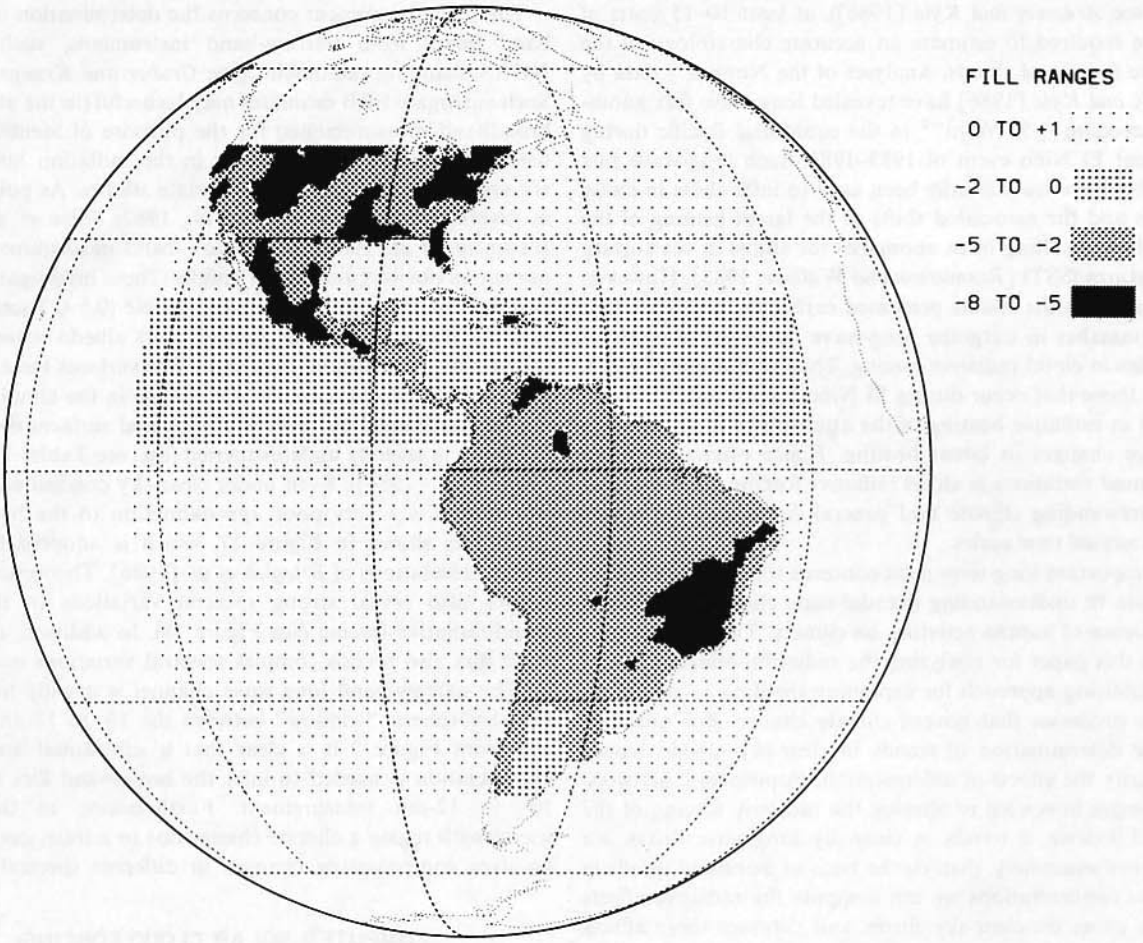

Fig. 17. Difference between computed visible (0.5–0.7 μm) and computed broadband (0.1–4 μm) clear-sky albedos for November, noontime conditions (source: *Briegleb et al.* [1986]).

scenes are chosen, by selecting scenes for which the spatial variance of the radiance is less than 1%. The variance is computed for 4 pixels that are adjacent to the pixel of interest. Preliminary results from the study show considerable promise for this approach.

Clear-sky fluxes. While comparison of the radiances serves to verify radiation codes, comparison of fluxes and albedos (for solar) on a global scale would verify the input for models and the parameterizations or various processes in models. As an example, the study of *Briegleb et al.* [1986] compared computed clear-sky albedos with the broadband albedos that were inferred from GOES measurements. The results of this study are shown in Figures 16*a*, 16*b*, and 16*c* for GOES-inferred, computed, and computed minus GOES-inferred values, respectively. The computations were performed on a $1° \times 1°$ grid, employing 10 vegetation types and surface- and aircraft-based observations for surface albedos. Comparisons, such as those shown in Figure 16 help verify or identify deficiencies in the following key aspects of model parameterizations: (1) zenith angle dependence of ocean and land albedos; (2) the climate model practice of specifying bulk albedos for large areas (10^2–10^3 km)^2, with complex vegetation types varying from tall trees to grass and shrubland, and (3) the approach of parameterizing surface albedos based on isolated measurements. For example, *Payne*'s [1972] extensive observations over the coastal waters of the Atlantic are generally adopted in climate models for ocean albedos. The ERBE data would facilitate comparisons similar to those shown in Figure 16 for the whole globe for both long-wave flux and albedo.

Cloud forcing. The final step is, of course, to compare cloud forcing generated by GCMs with observations. Such a comparison accomplishes the important objective of validating the radiative forcing simulated by GCMs. By itself, such a comparison will not lead to a verification of the cloud parameterization in GCMs. For a verification of the parameterization, data for cloud cover and cloud optical properties are needed in addition to radiation budget data.

4. Concluding Remarks Concerning the Future

It is appropriate at this stage to comment on the scientific needs for continuing ERB measurement into the future decades. The most important and immediate need concerns the accurate determination of cloud effects on climate and the general circulation. The determination of the clear-sky fluxes and the cloud forcing from ERB data on an operational basis commenced with ERBE (launched in late 1984) and, in view of the strong interannual variability of radiation fluxes (for ex-

ample, see *Ardanuy and Kyle* [1986]), at least 10–15 years of data are required to estimate an accurate climatology of the radiative forcing of clouds. Analyses of the Nimbus 7 data by *Ardanuy and Kyle* [1986] have revealed long-wave flux anomalies exceeding ± 50 W m^{-2} in the equatorial Pacific during the recent El Niño event of 1982–1983. Such long-wave flux anomalies have traditionally been used to infer shifts in cloud patterns and the associated shifts in the latent heating of the atmosphere resulting from anomalies (or shifts) in sea surface temperatures (SST) [*Rasmusson and Wallace*, 1983]. However, it is clear from the results presented earlier in this paper that huge anomalies in outgoing long-wave fluxes are a result of anomalies in cloud radiative forcing. Thus alterations of SSTs, such as those that occur during El Niño events, result in large changes in radiative heating of the atmosphere in addition to the large changes in latent heating. Hence estimates of the interannual variations in cloud radiative forcing are important for understanding climate and general circulation variations on interannual time scales.

The important long-term need concerns the potential role of ERB data in understanding decadal-scale climate trends and the influence of human activities on climate. The strategy outlined in this paper for analyzing the radiation budget offers a very promising approach for exploiting the data to shed light into the processes that govern climate change. For example, accurate determination of trends in clear-sky albedo would help clarify the effects of deforestation, tropospheric aerosols, and changes in sea ice in altering the radiative forcing of the planet. Likewise, if trends in clear-sky long-wave fluxes are determined accurately, then on the basis of measured trends in trace gas concentrations we can compute the radiative effects of trace gases on clear-sky fluxes and subtract these effects from measured trends to infer the relationship between changes in fluxes and temperatures, i.e., the long-wave feedback parameter. Finally, long-term variations in the cloud forcing would yield directly and straightforwardly the as yet mysterious contribution of cloud feedback to climate sensitivity. Thus continuation of accurate radiation budget measurements on decadel time scales is a mandatory objective for a quantitative understanding of climate sensitivity and for identifying the role of human activities on climate. It should also be mentioned that it is absolutely necessary for ERB instrument packages to routinely monitor the solar insolation.

The method proposed here for estimating the cloud forcing from ERB data is only the first step towards solving the cloud feedback problem. The present method helps establish the magnitude and the nature of the cloud radiative feedback from an observational view point. The next step is to understand how the cloud-radiative forcing and its variations are related to cloud cover and other atmospheric parameters, such as temperature and humidity.

The following comments are in order with respect to measurement strategies. The first comment concerns surface fluxes. As mentioned earlier, in order to understand the role of clouds in the general circulation, one needs to separate the cloud forcing of the column, the quantity that is measured by space-borne ERB instruments, in terms of its effect on the surface and on the troposphere. For this purpose, estimates of surface fluxes are essential. Surface radiation fluxes are also essential for determining the ocean and land energy budget. Thus future ERB studies should include determination of surface radiation fluxes as part of the observational program.

The second comment concerns the determination of broadband fluxes from narrow-band instruments, such as the NOAA scanning radiometer [see *Gruber and Krueger*, 1984]. Such surrogate ERB estimates may be useful (in the absence of broadband measurements) for the purpose of identifying the nature of interannual variability in the radiation budget but are unsuitable for quantitative climate studies. As pointed out in several studies [e.g., *Cess et al.*, 1982; *Shine et al.*, 1984; *Hartmann et al.*, 1986], the narrow-band measurements have numerous obvious and subtle pitfalls. These investigators have pointed out that the narrow-band visible (0.5–0.7 μm) albedo severely overestimates the (broadband) albedo when clouds are present. In addition, over snow-free surfaces the change in planetary albedo as a result of a change in the cloud cover is also overestimated but over snow-covered surfaces the change in albedo is severely underestimated (e.g., see Tables 1 and 2 of *Shine et al.*, [1984]). Even under clear-sky conditions, the visible albedo is a very poor approximation to the broadband albedo, as shown in Figure 17, which is adopted from the model calculations of *Briegleb et al.* [1986]. Theoretical calculations also reveal strong spectral variations in the solar cloud-radiative forcing (see Figure 18). In addition, the long-wave flux also reveals complex spectral variations (see Figure 2). The narrow-band long-wave channel is usually located in the atmospheric "window" between the 10- to 12-μm region, and from Figure 2 it is clear that a substantial amount of extrapolation is needed to infer the broadband flux from the 10- to 12-μm measurement. Furthermore, in the long-wavelength region a climate change due to a trace gas increase involves compensating changes in different spectral regions

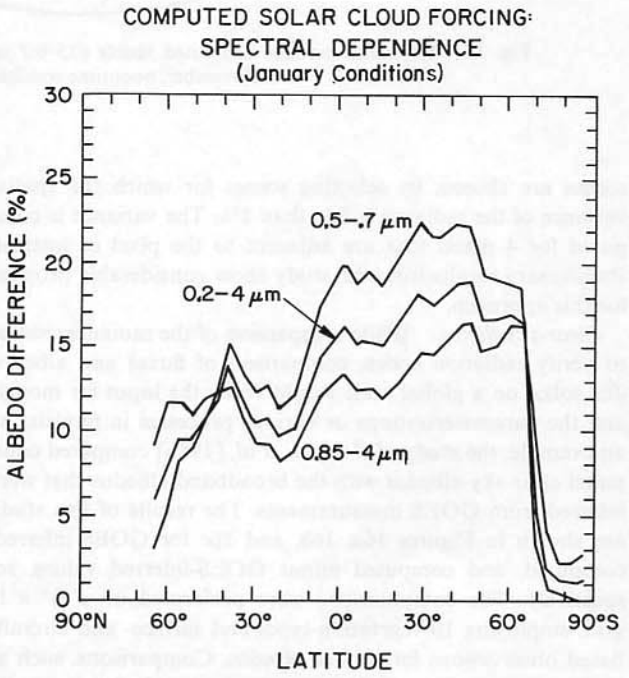

Fig. 18. Computed spectral variations in cloud-radiative forcing in the absorbed solar radiation for January conditions. The results were obtained by inserting a delta-Eddington scattering code for clouds and clear-sky in the GCM described by *Pitcher et al.* [1983]. The spectral variations in surface albedo are as specified by *Briegleb and Ramanathan* [1982] (source: B. P. Briegleb and V. Ramanathan, unpublished manuscript, 1984). The cloud-forcing terms in the visible (0.5–0.7 μm), broadband (0.2–4 μm), and the near infrared (0.85–4 μm) are shown.

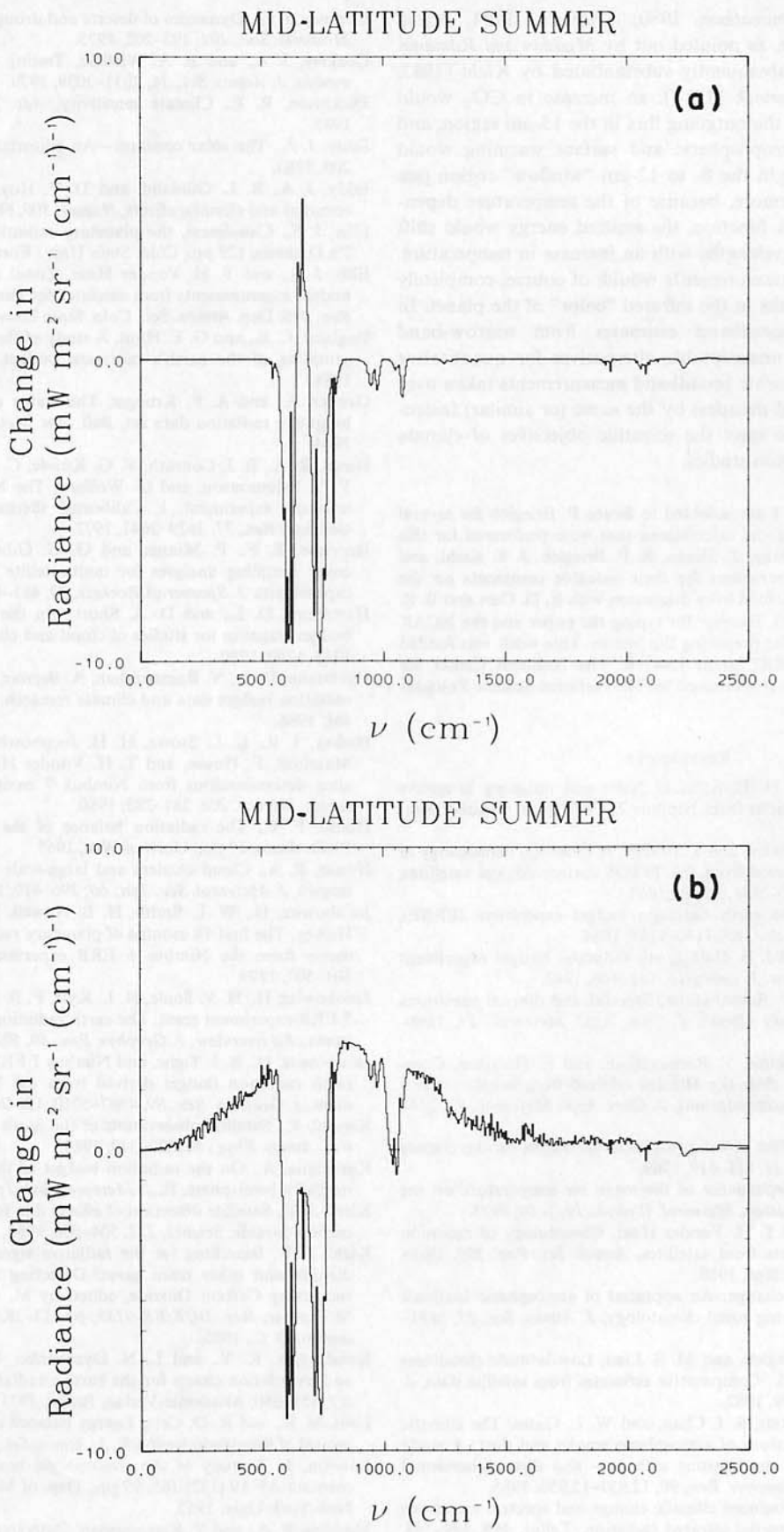

Fig. 19. Computed change in the top of the atmosphere radiance due to CO_2 doubling. The radiance change is computed by a 5 cm^{-1} narrow-band model and includes the direct radiative effects of CO_2 increase and the effects of temperature changes. (*a*) CO_2 increase alone. (*b*) CO_2 increase plus temperature change (source: *Kiehl* [1985]).

[*Madden and Ramanathan*, 1980; *Charlock*, 1984; *Kiehl*, 1985]. For example, as pointed out by *Madden and Ramanathan* [1980] and subsequently substantiated by *Kiehl* [1983, 1985], and by *Charlock* [1984], an increase in CO_2 would cause a decrease in the outgoing flux in the 15-μm region, and the CO_2-induced tropospheric and surface warming would lead to an increase in the 8- to 12-μm "window" region (see Figure 19). Furthermore, because of the temperature dependence of the Planck function, the emitted energy would shift towards shorter wavelengths with an increase in temperature. The narrow-band measurements would, of course, completely miss such subtle shifts in the infrared "color" of the planet. In summary then, boradband estimates from narrow-band measurements are unacceptable alternatives for quantitative climate studies; accurate broadband measurements taken over a long term (several decades) by the same (or similar) instrument are needed to meet the scientific objectives of climate and general circulation studies.

Acknowledgments. I am indebted to Bruce P. Briegleb for several of the graphics and model calculations that were performed for this paper. I thank A. Arking, T. Slingo, B. P. Briegleb, J. T. Kiehl, and the two anonymous reviewers for their valuable comments on the manuscript. I also benefited from discussion with R. D. Cess and B. R. Barksktrom. I thank G. Escobar for typing the paper and the NCAR graphics department for preparing the figures. This work was funded in part by NASA ERBE grant L9477B. The National Center for Atmospheric Research is sponsored by The National Science Foundation.

REFERENCES

Ardanuy, P. E., and H. L. Kyle, El Niño and outgoing longwave radiation: Observations from Nimbus 7, ERB, *Mon. Weather Rev.*, *114*, 415–433, 1986.

Bandeen, W. R., M. Halev, and J. Strange, A radiation climatology in the visible and infrared from the TIROS meteorological satellites, *NASA Tech. Note D-2534*, 30 pp., 1965.

Barkstrom, B. R., The earth radiation budget experiment (ERBE), *Bull. Am. Meteorol. Soc.*, *65*, 1170–1185, 1984.

Barkstrom, B. R., and J. B. Hall, Earth radiation budget experiment (ERBE): An overview, *J. Energy*, *6*, 141–146, 1982.

Briegleb, B. P., and V. Ramanathan, Spectral and diurnal variations in clear-sky planetary albedo, *J. Clim. Appl. Meteorol.*, *21*, 1168–1171, 1982.

Briegleb, B. P., P. Minnis, V. Ramanathan, and E. Harrison, Comparison of regional clear-sky albedos inferred from satellite observations and model computations, *J. Clim. Appl. Meteorol.*, *25*, 214–226, 1986.

Budyko, M. I., The effect of solar radiation variations on the climate of the earth, *Tellus*, *21*, 611–619, 1969.

Budyko, M. I., The dependence of the mean air temperature on the change of solar radiation, *Meteorol. Hydrol.*, *10*, 1–10, 1975.

Campbell, G. G., and T. H. Vonder Haar, Climatology of radiation budget measurements from satellites, *Atmos. Sci. Pap. 323*, Colo. State Univ., Fort Collins, 1980.

Cess, R. D., Climate change: An appraisal of atmospheric feedback mechanisms employing zonal climatology, *J. Atmos. Sci.*, *33*, 1831–1843, 1976.

Cess, R. D., B. P. Briegleb, and M. S. Lian, Low-latitude cloudiness and climate feedback: Comparative estimates from satellite data, *J. Atmos. Sci.*, *39*, 53–59, 1982.

Cess, R. D., G. L. Potter, S. J. Chan, and W. L. Gates, The climatic effects of large injections of atmospheric smoke and dust: A study of climate feedback mechanisms with one- and three-dimensional climate models, *J. Geophys. Res.*, *90*, 12,937–12,950, 1985.

Charlock, T. P., CO_2-induced climatic change and spectral variations in the outgoing terrestrial infrared radiation, *Tellus*, *36B*, 139–148, 1984.

Charlock, T. P., and V. Ramanathan, The albedo field and cloud radiative forcing produced by a general circulation model with internally generated cloud optics, *J. Atmos. Sci.*, *42*, 1408–1429, 1985.

Charney, J. G., Dynamics of deserts and drought in the Sahel, *Q. J. R. Meteorol. Soc.*, *101*, 193–202, 1975.

Coakley, J. A., and B. A. Wielicki, Testing energy balance climate models, *J. Atmos. Sci.*, *36*, 2031–2039, 1979.

Dickinson, R. E., Climate sensitivity, *Adv. Geophys.*, *28A*, 99–129, 1985.

Eddy, J. A., The solar constant—An editorial, *Clim. Change*, *5*, 207–209, 1983.

Eddy, J. A., R. L. Gilliland, and D. V. Hoyt, Changes in the solar constant and climatic effects, *Nature*, *300*, 689–693, 1982.

Ellis, J. S., Cloudiness, the planetary radiation budget and climate, Ph.D. thesis, 129 pp., Colo. State Univ., Fort Collins, 1978.

Ellis, J. S., and T. H. Vonder Haar, Zonal average earth radiation budget measurements from satellites for climate studies, *Atmos. Sci. Rep*, *240*, Dep. Atmos. Sci., Colo. State Univ., Fort Collins, 1976.

England, C. E., and G. E. Hunt, A study of the errors due to temporal sampling of the earth's radiation budget, *Tellus*, *36B*, 303–316, 1984.

Gruber, A., and A. F. Krueger, The status of the NOAA outgoing longwave radiation data set, *Bull. Am. Meteorol. Soc.*, *65*, 958–962, 1984.

Hanel, R. A., B. J. Conrath, V. G. Kunde, C. Prabahakara, I. Revah, V. V. Salomonson, and G. Wolford, The Nimbus 4 infrared spectrascopy experiment, 1, Calibrated thermal emission spectra, *J. Geophys. Res.*, *77*, 2629–2641, 1972.

Harrison, E. F., P. Minnis, and G. G. Gibson, Orbital and cloud cover sampling analyses for multisatellite earth radiation budget experiments, *J. Spacecraft Rockets*, *20*, 491–495, 1983.

Hartmann, D. L., and D. A. Short, On the use of earth radiation budget statistics for studies of cloud and climate, *J. Atmos. Sci.*, *37*, 1233–1250, 1980.

Hartmann, D. L., V. Ramanathan, A. Berroir, and G. E. Hunt, Earth radiation budget data and climate research, *Rev. Geophys.*, *24*, 439–468, 1986.

Hickey, J. R., L. L. Stowe, H. H. Jacobowitz, P. Pellegrino, R. H. Maschoff, F. House, and T. H. Vonder Haar, Initial solar irradiance determinations from Nimbus 7 cavity radiameter measurements, *Science*, *208*, 281–283, 1980.

House, F. B., The radiation balance of the earth from a satellite, Ph.D. thesis, 69 pp., Univ. of Wis., 1965.

Houze, R. A., Cloud clusters and large-scale vertical motions in the tropics, *J. Meteorol. Soc. Jpn.*, *60*, 396–410, 1982.

Jacobowitz, H., W. L. Smith, H. B. Howell, F. W. Nogle, and J. R. Hickey, The first 18 months of planetary radiation budget measurements form the Nimbus 6 ERB experiment, *J. Atmos. Sci.*, *36*, 501–507, 1979.

Jacobowitz, H., H. V. Soule, H. L. Kyle, F. B. House, and the Nimbus 7 ERB experiment team, The earth radiation budget (ERBE) experiment: An overview, *J. Geophys. Res.*, *89*, 5021–5038, 1984*a*.

Jacobowitz, H., R. J. Tighe, and Nimbus 7 ERB experiment team, The earth radiation budget derived from the Nimbus 7 ERB experiment, *J. Geophys. Res.*, *89*, 4997–5010, 1984*b*.

Kandel, R., Satellite observation of the earth radiation budget, *Contrib. Atmos. Phys.*, *56*, 322–340, 1983.

Katayama, A., On the radiation budget of the troposphere over the northern hemisphere, II, *J. Meteorol. Soc. Jpn.*, *45*, 1–25, 1967.

Kiehl, J. T., Satellite detection of effects due to increased atmospheric carbon dioxide, *Science*, *222*, 504–506, 1983.

Kiehl, J. T., Searching for the radiative signal of increasing carbon dioxide and other trace gases, Detecting the Climatic Effects of Increasing Carbon Dioxide, edited by M. C. MacCracken and F. M. Luther, *Rep. DOE/ER-0235*, pp. 13–28, *Dep. of Energy*, Washington, D. C., 1985.

Kondratyev, K. Y., and L. N. Dyachenko, Comparison of satellite and calculation charts for the earth's radiation budget, *Space Res.*, *XI*, 651–660, Akademie-Verlaq, Berlin, 1971.

Lian, M. S., and R. D. Cess, Energy balance climate models: A reappraisal of ice-albedo feedback, *J. Atmos. Sci.*, *34*, 1048–1062, 1977.

London, J., A study of the atmospheric heat balance, final report, contract AF 19 (122)-165, 99 pp., Dep. of Meteorol. and Oceanogr., New York Univ. 1957.

Madden, R. A., and V. Ramanathan, Detecting climate change due to increasing carbon dioxide, *Science*, *209*, 763–768, 1980.

Manabe, S., and R. T. Wetherald, Thermal equilibrium of the atmosphere with a given distribution of relative humidity, *J. Atmos. Sci.*, *24*, 241–259, 1967.

Minnis, P., and E. F. Harrison, Diurnal variability of regional cloud and clear-sky radiative parameters derived from GOES data, III, November 1978 radiative parameters, *J. Clim. Appl. Meteorol., 23*, 1032–1051, 1984.

Oerlemans, J., and H. M. Vanden Dool, Energy balance climate models: Stability experiments with a refined albedo and updated coefficients for infrared emission, *J. Atmos. Sci., 35*, 371–381, 1978.

Ohring, G., and P. Clapp, The effect of changes in cloud amount on the net radiation at the top of the atmosphere, *J. Atmos. Sci., 37*, 447–454, 1980.

Ohring, G., and A. Gruber, Satellite radiation observations and climate theory, *Adv. Geophys., 25*, 237–304, 1983.

Oort, A. H., and T. H. Vonder Haar, On the observed annual cycle in the ocean-atmosphere heat balance over the northern hemisphere, *J. Phys. Oceanogr., 6*, 781–800, 1976.

Payne, R. E., Albedo of the sea surface, *J. Atmos. Sci., 29*, 959–970, 1972.

Pitcher, E. J., R. C. Malone, V. Ramanathan, M. L. Blackmon, K. Puri, and W. Bourke, January and July simulations with a spectral general circulation model, *J. Atmos. Sci., 40*, 580–604, 1983.

Ramanathan, V., Radiative transfer within the earth's troposphere and stratosphere: A simplified radiative–convective model, *J. Atmos. Sci., 33*, 1330–1340, 1976.

Ramanathan, V., Interactions between ice-albedo, lapse-rate and cloud-top feedbacks: An analysis of the nonlinear response of a GCM climate model, *J. Atmos. Sci., 34*, 1885–1897, 1977.

Ramanathan, V., Modeling studies of cloud radiation feedback problems in the earth's atmosphere, paper presented at The Seymour Hess Memorial Symposium on Recent Advances in Planetary Meteorology, XVIII General Assembly, Int. Union of Geod. and Geophys., Hamburg, Germany, Aug. 15–27, 1983.

Ramanathan, V., Scientific use of surface radiation budget data for climate studies, *World Climate Programme Report on Surface Radiation Budget for Climate Applications*, Appendix B., pp. 1–30, edited by J. T. Sottles and G. Ohring, World Meteorological Organization, Geneva, Switzerland, 1985.

Ramanathan, V., and R. E. Dickinson, A scheme for forming nonprecipitating low-level clouds in GEMS, in *Clouds in Climate: Modeling and Satellite Observational Studies*, pp. 85–87, NASA Goddard Institute for Space Studies, New York, 1981.

Ramanathan, V., and P. Downey, An approach for verifying clear-sky radiation models with ERBS Scanner measurements, paper presented at Radiation Symposium, Am. Meteorol. Soc., May 1986.

Ramanathan, V., E. J. Pitcher, R. C. Malone, and M. L. Blackmon, The response of a spectral general circulation model to refinements in radiative processes, *J. Atmos. Sci., 180*, 605–630, 1983.

Raschke, E., and W. R. Bandeen, The radiation balance of the planet earth from radiation measurements of the satellite Nimbus II, *J. Appl. Meteorol., 9*, 215–238, 1970.

Rasmusson, E. M., and J. M. Wallace, Meteorological aspects of the El Niño/Southern oscillation, *Science, 222*, 1195–1202, 1983.

Rasool, S. I., and C. Prabhakara, Heat budget of the southern hemisphere, *Problems of Atmospheric Circulation*, pp. 76–92, Spartan, Washington, D. C., 1966.

Schneider, S. H., and C. Mass, Volcanic dust, sunspots and temperature trends, *Science, 190*, 741–746, 1975.

Sellers, W. D., A global climate model based on the energy balance of the earth-atmosphere system, *J. Appl. Meteorol., 8*, 392–400, 1969.

Shine, K. P., A. Henderson-Sellers, and A. Slingo, The influence of the spectral response of satellite sensors on estimates of broadband albedo, *Q. J. R. Meteorol. Soc., 110*, 1170–1179, 1984.

Shukla, J., and Y. Sud, Effect of cloud-radiation feedback on the climate of a general circulation model, *J. Atmos. Sci., 38*, 2337–2353, 1981.

Slingo, J., A study of the earth's radiation budget using a general circulation model, *Q. J. R. Meteorol. Soc., 108*, 379–405, 1982.

Smith, L. A., Radiative forcing of the southwest summer monsoon, Ph.D. thesis, 520 pp., Colo. State Univ., Fort Collins, 1984.

Stephens, G. L., G. G. Campbell, and T. H. Vonder Haar, Earth radiation budget measurements from satellites and their interpretation for climate modeling and studies, *J. Geophys. Res., 86*, 9739–9760, 1981.

Suomi, V. E., K. J. Hanson, and T. H. Vonder Haar, The theoretical basis for low-resolution radiameter measurements from a satellite, annual report, grant WBG-27, pp. 79–100, Dep. of Meteorol., Univ. of Wis., 1967.

Vonder Haar, T. H., Variations of the earth's radiation budget, Ph.D. thesis, 118 pp., Univ. of Wis., 1968.

Vonder Haar, T. H., and A. H. Oort, New estimate of annual poleward energy transport by northern hemisphere oceans, *J. Phys. Oceanogr., 3*, 169–172, 1973.

Vonder Haar, T. H., and V. E. Suomi, Satellite observations of the earth's radiation budget, *Science, 163*, 667–669, 1969.

Vonder Haar, T. H., and V. E. Suomi, Measurements of the earth's radiation budget from satellites during a five-year period, Extended time and space means, *J. Atmos. Sci., 28*, 305–314, 1971.

Warren, S. G., and S. H. Schneider, Seasonal simulation as a test for uncertainties in parameterizations of a Budyko-Sellers zonal climate model, *J. Atmos. Sci., 36*, 1377–1391, 1979.

Wetherald, R. T., and S. Manabe, The effects of changing the solar constant on the climate of a general circulation model, *J. Atmos. Sci., 32*, 2044–2059, 1975.

Wilson, R. C., Measurements of solar total irradiance and its variability, *Space Sci.* Rev., *38*, 203–242, 1984.

V. Ramanathan, Department of Geophysical Sciences, University of Chicago, 5734 S. Ellis Avenue, Chicago, IL 60637.

(Received February 21, 1986;
revised August 5, 1986;
accepted August 12, 1986.)